DMD Fast Forward. Published on November 25, 2015 as DOI: 10.1124/dmd.115.066852
This article has not been copyedited and formatted. The final version may differ from this version.

Cynomolgus Monkey as a Clinically Relevant Model to Study Transport Involving Renal Organic Cation Transporters: *In Vitro* and *In Vivo* Evaluation

Hong Shen, Tongtong Liu, Hao Jiang, Craig Titsch, Kristin Taylor, Hamza Kandoussi, Xi Qiu, Cliff Chen, Sunil Sukrutharaj, Kathy Kuit, Gabe Mintier, Prasad Krishnamurthy, R. Marcus Fancher, Jianing Zeng, A. David Rodrigues, Punit Marathe, and Yurong Lai

Department of Metabolism and Pharmacokinetics (H.S., T.L., X.Q., C.C., R.M.F., A.D.R., P.M., Y.L.), Department of Bioanalytical Sciences (H.J., C.T., K.T., H.K., J.Z.), Bristol-Myers Squibb Research and Development, Princeton, NJ; Department of Genomic Technologies (K.K.) and Department of Genome Biology (G.M.), Bristol-Myers Squibb Research and Development, Pennington, NJ; Department of Molecular Biology (S.S., P.K.), Bristol-Myers Squibb Biocon R&D Center, Bangalore, India

Running title: Use of Monkey to Assess Transport by OCT2 and MATEs

Corresponding author and contact information:

Hong Shen, Ph.D.

Bristol-Myers Squibb Company

F1.3802, Route 206 & Province Line Road

Princeton, NJ 08543-4000

E-mail: hong.shen1@bms.com

Tel: (609) 252-4509

Fax: (609) 252-6802

Number of text pages: 29

Number of tables: 5

Number of figures: 7

Number of references: 56

Number of words:

Abstract: 244

Introduction: 754

Discussion: 1,550

Abbreviations: *AUC*, area under the concentration-time curve; C_{max}, maximum plasma concentration; cMATE1, cynomolgus multidrug and toxin extrusion protein 1; cMATE2K, cynomolgus kidney-specific multidrug and toxin extrusion protein 2; CMD, cimetidine; cOCT2,

cynomolgus organic cation transporter 2; CI, confidence interval; *CL*, clearance; CL_R, renal clearance; DDI, drug-drug interaction; E3S, estrone-3-sulfate; HBSS, Hank's balanced salt solution; HEK 293: human embryonic kidney 293 cells; hMATE1, human multidrug and toxin extrusion protein 1; hMATE2K, human kidney-specific multidrug and toxin extrusion protein 2; hOCT2, human organic cation transporter 2; IC_{50}, concentration of inhibitor required for 50% inhibition of transport; IPM, imipramine; K_t, Michaelis-Menten constant that corresponds to the substrate concentration at which the transport rate is half of V_{max}; KCZ, ketoconazole; LC-MS/MS, liquid chromatography coupled with tandem mass spectrometry; MFM, metformin; MPP^+, 1-methyl-4-phenylpyridinium; MRM, multiple reaction monitoring; MTX, methotrexate; PYR, pyrimethamine; QC, quality control; QD, quinidine; $T_{1/2}$, apparent terminal half-life; T_{max}, time to reach maximal plasma concentration; TEA, tetraethylammonium; VDN, vandetanib; V_{max}, maximum uptake rate; V_{ss}, steady-state volume of distribution.

Abstract

Organic cation transporter (OCT) 2, multidrug and toxin extrusion protein (MATE) 1, and MATE2K mediate the renal secretion of various cationic drugs and can serve as the loci of drug-drug interactions (DDI). To support the evaluation of cynomolgus monkey as a surrogate model for studying human organic cation transporters, monkey genes were cloned and shown to have a high degree of amino acid sequence identity versus their human counterparts (93.7%, 94.7%, and 95.4% for OCT2, MATE1 and MATE2K, respectively). Subsequently, the 3 transporters were individually stably expressed in human embryonic kidney (HEK) 293 cells and their properties (substrate selectivity, time course, pH-dependence, and kinetics) were found to be comparable to the corresponding human form. For example, six known human cation transporter inhibitors, including pyrimethamine (PYR), showed generally similar IC_{50} values against the monkey transporters (within 6-fold). Consistent with the in vitro inhibition of metformin (MFM) transport by PYR (IC_{50} for cynomolgus OCT2, MATE1 and MATE2K; 1.2 ± 0.38, 0.17 ± 0.04 and 0.25 ± 0.04 μM, respectively), intravenous pretreatment of monkeys with PYR (0.5 mg/kg) decreased the clearance (54 ± 9%) and increased in the area under the plasma concentration-time curve of MFM (AUC ratio versus control = 2.23; 90% confidence interval of 1.57 to 3.17). These findings suggest that the cynomolgus monkey may have some utility in support of in vitro-in vivo extrapolations (IVIVEs) involving the inhibition of renal OCT2 and MATEs. In turn, cynomolgus monkey-enabled IVIVEs may inform human DDI risk assessment.

DMD Fast Forward. Published on November 25, 2015 as DOI: 10.1124/dmd.115.066852
This article has not been copyedited and formatted. The final version may differ from this version.

Introduction

It is widely appreciated that renal elimination of cations, drug-, toxin- or endogenous metabolite-related, is achieved not only by glomerular filtration but also by active transport processes that facilitate their tubular secretion and reabsorption. Indeed, the mechanisms governing the renal elimination of organic cations have been studied in detail, and the transporters facilitating their tubular uptake and extrusion have been identified (Okuda et al., 1996, Otsuka et al., 2005, Masuda et al., 2006).

Secretion of organic cations in renal proximal tubules involves at least two distinct transporters, located in the basolateral and apical membranes of proximal tubule cells (Motohashi et al., 2002, Masuda et al., 2006, Motohashi et al., 2013). Specifically, organic cations, like metformin (MFM), 1-methyl-4-phenylpyridinium (MPP^+), tetraethylammonium (TEA), and cimetidine (CMD), are taken up from the circulation by organic cation transporter 2 (OCT2) expressed on the basolateral domain of renal proximal tubular cells. In turn, uptake is followed by efflux into the tubular fluid by multidrug and toxin extrusion protein (MATE) 1 and MATE2K expressed on the apical domain of the same cells. Therefore, OCT2 and MATEs function coordinately to mediate vectorial transport of certain cationic drugs, from blood to tubular fluid, which represents the tubular secretion clearance component of total renal clearance.

Perturbation of cation transport function, because of modulation by drugs or polymorphisms, can lead to drug-drug interactions (DDIs) and exacerbated drug-induced renal toxicity (Fisel et al., 2014). Although less than a 3-fold change in systemic exposure of victim drug is typically reported, the concentrations of drug in the kidney can be dramatically increased because of inhibition of efflux. It is possible to envision altered efficacy and toxicity in such a scenario. Consequently, *in vitro* studies using various transporter expression systems are

routinely performed to evaluate whether a new molecular entity is an inhibitor or substrate of human renal organic cation transporters. Such studies can be performed preclinically, or after dosing of the new molecular entity to human subjects, and are widely accepted by pharmaceutical companies and regulatory authorities in support of DDI and drug-induced nephrotoxicity risk assessment (Okuda et al., 1999, International Transporter et al., 2010, Morrissey et al., 2013) (US FDA 2012; European Medicines Agency 2012). In fact, there is a need to integrate, understand, and translate the *in vitro* data in support of risk assessment prior to human dosing, or prioritize specific types of clinical DDI studies. To date, however, examples of IVIVEs for DDIs involving renal transporters, such as OCTs and MATEs, are few in number.

Increasingly, investigators are leveraging a combination of *in vitro* and *in vivo* animal (e.g., humanized rodents and non-human primates) data to support IVIVE involving the inhibition of drug-metabolizing enzymes (e.g., cytochrome P450 3A4) and transporters (e.g., organic anion transporting polypeptide) (Tang and Prueksaritanont, 2010, Shen et al., 2013, Jaiswal et al., 2014). When successful, appropriately characterized and validated animal models can provide mechanistic insight, support modeling, and enable IVIVE exercises. Obviously, one has to consider species differences in genetics, substrate specificity, tissue distribution and abundance of transporters and enzymes. For example, OCT2 expression in human and monkey kidney tissue is similar. In comparison, both Oct1 and Oct2 are expressed in mouse and rat kidney although the expression levels relative to that of human OCT2 are unknown (Urakami et al., 1998, Motohashi et al., 2002, Alnouti et al., 2006, Bleasby et al., 2006). Conversely, MATE1 and MATE2K are known to be highly expressed in human kidney but the counterpart of human MATE2K has not been identified in rats and mice (Otsuka et al., 2005, Masuda et al., 2006). This has led some to question the utility of rodent models. On the other hand, the cynomolgus

monkey has been considered a more appropriate animal model to assess DDIs involving renal clearance. However, monkey OCT2, MATE1 and MATE2 have not been cloned and characterized.

The aim of the present study was to assess the applicability of cynomolgus monkey as a suitable surrogate preclinical model for studying OCT2-, MATE1- and MATE2K-mediated DDIs. It was possible to clone full-length cynomolgus monkey OCT2, MATE1 and MATE2K (cOCT2, cMATE1 and cMATE2K), and establish stably transfected cell lines for each of the 3 transporters. In turn, the *in vitro* profile of each transporter (substrate specificity, time course, pH-dependence, transport kinetics and inhibition profile) was characterized and compared to that of the corresponding human form. The effort was extended to include an *in vivo* monkey DDI study, employing pyrimethamine (PYR) as perpetrator and MFM as victim, and the results were compared to those of literature reports involving human subjects.

DMD Fast Forward. Published on November 25, 2015 as DOI: 10.1124/dmd.115.066852
This article has not been copyedited and formatted. The final version may differ from this version.

Materials and Methods

Chemicals and Materials. [^{14}C]Metformin ([^{14}C]MFM; 98 mCi/mmol) and [^{3}H]methotrexate ([^{3}H]MTX 25.9 Ci/mmol) were purchased from Moravek Biochemicals, Inc. (Brea, CA). [^{3}H]N-methyl-4-phenylpyridinium ([^{3}H]MPP^{+}; 80 Ci/mmol), [^{14}C]tetraethylammonium ([^{14}C]TEA; 3.2 mCi/mmol), and [^{3}H]estrone-3-sulfate ([^{3}H]E3S; 45.6 Ci/mmol) were purchased from PerkinElmer Life and Analytical Sciences (Waltham, MA). [^{3}H]Cimetidine ([^{3}H]CMD; 24.4 Ci/mmol) was obtained from American Radiolabeled Chemicals (St. Louis, MO). Unlabeled MFM, PYR, CMD, quinidine (QD), vandetanib (VDN), ketoconazole (KCZ), and imipramine (IPM) were purchased from Toronto Research Chemicals Inc. (North York, ON). All other chemicals were of reagent grade and purchased from Sigma-Aldrich (St. Louis, MO). Human embryonic kidney (HEK 293) Flip-In cells and Lipofectamine 2000 transfection system were purchased from Invitrogen-Life Technologies (Carlsbad, CA). All cell culture media and reagents were obtained from Mediatech, Inc (Manassas, VA) or Life Technologies (Carlsbad, CA). Poly-D-lysine-coated 24-well plates were obtained from BD Biosciences (Bedford, MA). Sources of other materials are stated in individual method sections.

Cloning of cOCT2, cMATE1 and cMATE2K, Cell Culture, and Uptake Transport Studies. The cloning of cOCT2, cMATE1 and cMATE2K, and stable transfection in HEK 293 cells are described in detail in Supplementary Material section. The monkey transporter cDNA gene sequences were deposited in National Center for Biotechnology Information GenBank with accession numbers of KP731382, KP731383, and KP731384 for cOCT2, cMATE1 and cMATE2K, respectively.

All cells were grown in Dulbeccos's modified eagle's medium supplemented with 10% heat-inactivated fetal bovine serum, 0.1 mM non-essential amino acids, 2 mM L-glutamine, and

DMD Fast Forward. Published on November 25, 2015 as DOI: 10.1124/dmd.115.066852
This article has not been copyedited and formatted. The final version may differ from this version.

0.1 mg/mL Hygromycin B at 37°C in an incubator supplied with 5% CO_2. Subculture was performed every week, and passage numbers between 5 and 30 were used throughout the study to keep the transporter expression level and functional activity consistent.

The protocol for uptake experiments has been previously described (Shen et al., 2013). Briefly, HEK 293 cells were seeded into poly-D-lysine-coated 24-well plates at a density of 0.5 x 10^6 cells per well. Two to three days after seeding, cells were grown to confluence and uptake experiments were performed. Cells were washed twice with 1.5 mL Hanks' balanced salt solution (HBSS) pre-warmed at 37°C. The uptake study was initiated by adding 0.2 mL of pre-warmed standard buffer (HBSS containing 10 mM HEPES, pH 7.4 for OCT2, and pH 8.4 for MATE1 and MATE2K, respectively) containing radiolabeled compounds ([^{14}C]MFM or others). At the end of the incubation period, the buffer was removed and the cells in each well were rinsed thrice with 1 mL ice-cold HBSS (4°C). For a time course uptake study, the uptake of 2 μM [^{14}C]MFM was terminated at specific times by aspirating and rinsing. To measure the pH-dependent transport of MFM, the uptake of 1 μM [^{14}C]MFM in buffers at different pH (HBSS with 10 mM HEPES, and HCL and NaOH for adjusting to pH 5.0, 6.0, 7.0, 7.4, 8.0, 9.0, 10.0, and 11.0) was determined over 2 min. For the assessment of MFM transport kinetics, a constant amount of radiolabel with varying amounts of unlabeled substrate was used.

In order to assess the inhibitory potency of PYR, CMD, QD, VDN, KCZ, and IPM toward uptake of 2 μM [^{14}C]MFM by monkey and human organic cation transporters, the test compound at various concentration was added simultaneously with MFM. At 2 min (within the linear time range; Fig. 2), the buffer was removed to terminate the reaction and the cells were washed three times with ice-cold HBSS. After air-dried for at least 30 min in the fume hood, the cells were lysed with 0.3 mL of 0.1% Triton X-100, and the radioactivity was determined by

DMD Fast Forward. Published on November 25, 2015 as DOI: 10.1124/dmd.115.066852
This article has not been copyedited and formatted. The final version may differ from this version.

liquid scintillation counting. The protein concentrations in cell experiments were determined by the BCA method using bovine serum albumin as a standard (Pierce Chemical, Rockfold, IL).

Liquid Chromatography Coupled with Tandem Mass Spectrometry (LC-MS/MS) Quantification of OCT2, MATE1 and MATE2K Proteins in Transporter-Overexpressing Cells. Membrane protein fraction from transporter-overexpressing cells was extracted using ProteoExtract® Native Membrane Protein Extraction kit, as per the manufacturer's instructions (Calbiochem, San Diego, CA). Membrane protein fraction samples were digested as described previously (Qiu et al., 2013). In brief, all samples were adjusted to a maximum protein concentration of 2 mg/mL. Samples containing 40 to 200 µg membrane proteins were reduced with 10 mM dithiothreitol at 95°C for 5 min in 25 mM ammonium bicarbonate buffer with 1% deoxycholate. After cooling down, the membrane protein was then alkylated with 15 mM iodoacetamide in the dark for 30 min, followed by trypsin (trypsin/protein ratio: 1/50) digestion at 37°C for 16 h with shaking. To prepare calibration curves, the same amount of human serum albumin was digested followed the same procedure. The digestion was terminated by addition of an equal volume of water (with 0.2% formic acid) containing a fixed concentration of the synthetic stable isotope-labeled peptides (final concentration: 20 nM) that serves as an internal standard (IS). For construction of the calibration curve, an equal volume of water (with 0.2% formic acid) containing the IS (20 nM) and the synthetic unlabeled peptide standard (0.1-200 nM each). The samples were centrifuged at 14,000 x g for 10 min and the supernatant was filtered through Millipore filtration plate (Billerica, MA), dried and reconstituted in 100 µL 0.1% formic acid water.

Peptide quantification was performed using a Shimadzu Nexera UHPLC system (LC-30A; Columbia, MD) coupled with an API-6500 triple quadrupole mass spectrometer (ABSciex,

DMD Fast Forward. Published on November 25, 2015 as DOI: 10.1124/dmd.115.066852
This article has not been copyedited and formatted. The final version may differ from this version.

Foster City, CA). A sample volume of 20 µL was injected onto the column and the UHPLC separation was achieved using Waters BEH300 C18 2.1 x 100 mm Peptide Separation Technology column with a 1.7 µm particle size and 300 Å pore size (Milford, MA), and peptides were eluted with 0.3 mL/min of 0.1% formic acid in water (solvent A) and 0.1% formic acid in acetonitrile (solvent B) using the following gradient. The separation of peptides was achieved by the following linear gradients: 1 min, 5% solvent B; 8 min, 30% solvent B; 8.2 min, 90% solvent B; 10.2 min, 5% solvent B; 14 min controller stopped. Quality controls for the method were conducted in a sample spiked with a fixed concentration of a representative synthetic unlabeled peptide (14 nM). The accuracy (relative error) was less than 10% and precision (coefficient of variation) was less than 5% for all quality control samples (Qiu et al., 2013). All selected peptides and their optimized mass transitions with the highest sensitivity are specified in Table 1.

Pharmacokinetic Experiments Employing Cynomolgus Monkeys. All experiments with cynomolgus monkeys were performed in accordance with the National Institutes of Health guidelines and approved by Bristol-Myers Squibb Animal Care and Use Committee. The animals were housed in a temperature- and humidity-controlled room with a 12-h light/dark cycle. Pharmacokinetic experiments with MFM, either alone or in combination with PYR, were performed in male cynomolgus monkeys weighting between 5 to 7 kg (n = 3 and 2 animals per group for intravenous (IV) and oral administration (PO), respectively) in a crossover study design with a 1-week washout between treatments and the MFM alone treatment ahead of the coadministration treatment. Monkeys were fasted beginning the night before each oral but not IV dose of MFM or PYR. For intravenous application, MFM was dissolved in physiological saline and given by IV infusion via a femoral vein at 3.9 m/kg over 15 minutes (5 mL/kg). In IV co-

DMD Fast Forward. Published on November 25, 2015 as DOI: 10.1124/dmd.115.066852
This article has not been copyedited and formatted. The final version may differ from this version.

administration group, PYR dissolved in saline with 10% ethanol to obtain a concentration of 0.1 mg/mL, was also given by femoral vein infusion for 15 min at a dose of 0.5 mg/kg (7.5 mL/kg), 60 min before the administration of MFM. Animals receiving MFM alone were injected with an equivalent volume of vehicle (i.e., 7.5 mL/kg). For oral application, monkeys were given a single oral dose of 8.6 mg/kg MFM that was dissolved in saline by gavage (5 mL/kg). In oral co-administration group, each monkey also received an oral dose of 2.5 mg/kg PYR (5 mL/kg) as a suspension in saline with 10% ethanol, 60 min before the administration of MFM. Animals receiving MFM alone were orally administered with an equivalent volume of vehicle (i.e., 5 mL/kg). Approximately 500 micro-liter of arterial blood was collected in tubes containing potassium (K2) EDTA with vascular access port at 0, 0.25, 0.5, 0.45, 1, 2, 3, 5, 7, 24 and 48 hr (IV) after MFM administration. Plasma was generated by centrifugation at 10,000g for 3 min. Urine samples were collected during the following intervals: 0–7 hr, 7-24 hr and 24-48 hr after IV administration of 3.9 mg/kg MFM, and 0–3 hr, 3-6 hr and 6–24 hr after oral administration of 8.6 mg/kg MFM. The volume of urine obtained was recorded at the end of each collection interval. The plasma and urine samples were stored at -70°C until analysis within the known period of stability.

LC-MS/MS Measurement of Pharmacokinetic Samples. The plasma and urine specimens (100 µL) were mixed with 300 µL of acetonitrile containing 1% formic and 1 ng/mL of d6-metformin (internal standard). The mixed solutions were centrifuged at 2,000g for 5 min, and 300 µL of the supernatant was transferred to a clean 96-well plate. The supernatant was dried under nitrogen at 40°C until dry, reconstituted with 100 µL of 50 mM ammonium formate in acetonitrile/water (50/50, v/v, pH 3.2), and then injected (10 µL) to LC-MS/MS. A Triple Quad™ 5500 mass spectrometer (AB SCIEX, Foster City, CA) tandem with a Nexera LC-20

UHPLC system (Shimadzu Scientific Instruments Inc., Columbia, MD) was used for the LC-MS/MS analysis in the positive electrospray ionization and multiple reaction monitoring (MRM) mode. The chromatographic separation was achieved on a Zorbax 300-SCX column (3.0 mm x 50 mm, 5 µm; Agilent Technologies, Santa Clara, CA) under 40°C at a flow rate of 0.4 mL/min using an isocratic method. The mobile phase consisted of 50 mM ammonium formate in acetonitrile/water (50/50, v/v, pH 3.2). MFM, PYR, and d6-metformin were detected at MRM transitions of *m/z* 130.0 → 60.0, 249.1 → 177.1, and 136.1 → 60.0, respectively. The calibration standards and QC samples were prepared in charcoal-stripped plasma and urine which were absent of the analytes. The curves were linear in the range of 0.05–10 ng/mL (weighting 1/x2). Assay performance was evaluated using the QCs in terms of assay selectivity, precision (≤ 6%), and accuracy (≤ ± 15%).

Data Analysis. The data represent the results from a single in vitro study run in triplicate and a minimum of two experiments were performed. For example, supplemental Fig. 4 shows two experiments conducted for a single inhibition study. To estimate transport kinetics parameters of MFM into cynomolgus monkey and human transporter-expressing HEK 293 cells, the transporter-mediated uptake was calculated by subtracting the uptake in mock-transfected cells from that in transporter-expressing HEK 293 cells. The following equation was used to estimate the parameters:

$$V = \frac{V_{\max} \text{ x} [S]}{K_t + [S]}; \qquad CL_{\text{int}} = \frac{V_{\max}}{K_t}$$

where V is the rate of uptake measured at the given concentration; V_{max} is the maximal rate of uptake; K_t represents the Michaelis-Menten constant at which the transport rate is half its maximal value; [S] is the substrate concentration, and CL_{int} is the intrinsic clearance.

For transporter inhibition studies, IC_{50} values, the concentration of inhibitor required for 50% inhibition of uptake, were calculated using the following equation:

$$y = 100\% \text{ x} \left(1 - \frac{I^{\gamma}}{I^{\gamma} + IC_{50}^{\gamma}} \right)$$

where y is percent of control (MFM uptake in the absence of inhibitor) at the given inhibitor concentration (I); γ is the Hill coefficient that describes steepness of inhibition curve. V_{max}, K_t and IC_{50} were determined by fitting data to the equations using Phoenix WinNonlin 6.3 (Certara, L.P.; St. Louis, MO).

For pharmacokinetic analysis, the noncompartmental analyses of MFM and PYR plasma concentration-time data were performed to estimate the area under the plasma concentration-time curve (AUC), clearance (CL), steady-state volume of distribution (V_{ss}), apparent terminal half-life ($T_{1/2}$), maximal plasma concentration (C_{max}), and the time to reach maximal plasma concentration (T_{max}) using Kinetica (Thermo Fisher Scientific, Waltham, MA). Renal clearance (CL_R) was calculated as the ratio of the cumulative urinary excretion (A_e; amount recovered in urine) to plasma AUC:

$$CL_R = \frac{A_e}{AUC}$$

Data are also reported as geometric mean ratio of MFM pharmacokinetic parameter in the presence of PYR versus absence of PYR. In each case, a two-sided 90% confidence interval

(90% CI) for the geometric mean ratio between the treatments was calculated. Unpaired or paired Student's *t*-test was applied according to the nature of each data set. Data were analyzed using Prism (GraphPad Software, Inc., San Diego, CA). A *p*-value of less than 0.05 was considered to be statistically significant (* $p < 0.05$, ** $p < 0.01$, and *** $p < 0.001$).

DMD Fast Forward. Published on November 25, 2015 as DOI: 10.1124/dmd.115.066852
This article has not been copyedited and formatted. The final version may differ from this version.

Results

Cloning of cOCT2, cMATE1 and cMATE2K. PCR primers based on the conserved nucleotide sequences just outside the coding frames of human, chimpanzee, and rhesus monkey OCT2, MATE1 and MATE2K were used to amplify full-length fragments from pooled cynomolgus monkey kidney cDNA. The nucleotide sequences of cOCT2, cMATE1, and cMATE2K are reported as GenBank Accession Numbers KP731382, KP731383, and KP731384, respectively. The derived amino acid sequences of cOCT2, cMATE1, and cMATE2K were found to be 93.7%, 94.7% and 95.4% identical, and 96.9%, 96.0% and 97.4% similar (i.e., substitution of residues with similar chemical and functional properties) to hOCT2, hMATE1 and hMATE2K reference sequences, respectively (Supplemental Fig. 1). In addition to the splice form that is orthologous to human MATE2K transcript (NM_001099646), a different splice isoform that omits exon 6, resulting in a loss of 15 amino acids (GenBank KP731385), was found in 2 out of 8 cMATE2K clones. No human equivalent for this splice form currently has been reported in National Center for Biotechnology Information GenBank. There was a single nucleotide discrepancy in 6 out of 7 cOCT2 clones, resulting in an amino acid difference (M194T) compared to the published human, chimpanzee, and rhesus monkey OCT2 sequences.

In order to characterize transport activity, the recombinant Flp-In expression vectors were prepared using the fragments of full-length cOCT2, cMATE1, and cMATE2K. The vectors were co-expressed with one containing Flp recombination target -integrating enzyme in HEK 293 cells by stable transfection. Positively transfected cells were selected by hygromycin B resistance and screening uptake of [^{3}H]MPP^{+} and [^{14}C]MFM. Increased expression of the monkey transporter was shown by dramatically enhanced expression of mRNA levels compared to the mock cells transfected with empty vector using reverse transcription polymerase chain reaction method

DMD Fast Forward. Published on November 25, 2015 as DOI: 10.1124/dmd.115.066852
This article has not been copyedited and formatted. The final version may differ from this version.

(data not shown). The transporter-overexpressing cell lines selected for further studies were then subjected to LC-MS/MS analysis to determine transporter protein content, and the results revealed comparable expression levels between cynomolgus monkey and human transporter transfected cell lines (monkey vs. human: 39.4 ± 1.4 vs. 58.7 ± 1.4, 347 ± 31.1 vs. 329 ± 30.8, 41.7 ± 3.7 vs. 18.6 ± 1.1 pmol/mg membrane protein for OCT2, MATE1 and MATE2K, respectively).

Transporter Activity in the Presence of cOCT2, cMATE1, and cMATE2K. To confirm that cOCT2, cMATE1, and cMATE2K proteins in the transfected HEK 293 cells were functionally active, uptake studies were conducted with 4 cationic drugs and 2 anionic drugs. Cellular uptake of the radio-labeled drugs was determined after 5 min of incubation and it was found that all three monkey transporters were active (versus mock cells) with MFM, MPP^+, TEA and CMD ($p < 0.001$; Figs 1A to 1D), similar to hOCT2 and hMATEs (Okuda et al., 1999, Kimura et al., 2005, Otsuka et al., 2005, Tahara et al., 2005, Tanihara et al., 2007, Zolk et al., 2009b). With the exception of E3S for hMATE2K (~2-fold versus mock cells), both monkey and human OCT2 and MATEs exhibited low uptake rates with E3S and MTX although some uptake rates are significantly greater than that in mock cells (Fig. 1).

cOCT2, cMATE1, and cMATE2K Exhibit Similar Time Course and pH-Dependent Transport of MFM as Compared to Human Organic Cation Transporters. To further examine functional activity of cOCT2, cMATE1, and cMATE2K, the time- and pH-dependence of MFM uptake was assessed also. In cOCT2-HEK and cMATE1-HEK cells, the uptake of [^{14}C]MFM was almost identical to that in hOCT2-HEK and hMATE1-HEK cells, respectively, was linear over 2 min and displayed a plateau after 5 min (Figs. 2A and 2B). Likewise, OCT2 and MATE1 protein expression levels are similar (less than 2-fold difference) between monkey

DMD Fast Forward. Published on November 25, 2015 as DOI: 10.1124/dmd.115.066852
This article has not been copyedited and formatted. The final version may differ from this version.

and human transporter transfected cell lines (i.e. monkey vs. human: 39.4 ± 1.4 vs. 58.7 ± 1.4 and 347 ± 31.1 vs. 329 ± 30.8 pmol/mg membrane protein for OCT2 and MATE1, respectively). In contrast, [^{14}C]MFM uptake rate by cMATE2K was approximately 2-fold higher than that by hMATE2K (Fig. 2C). In agreement, the transporter protein level was found to be about 2-fold greater in cMATE2K-HEK cells than in hMATE2K-HEK cells (41.7 ± 3.7 vs. 18.6 ± 1.1 pmol/mg membrane protein). [^{14}C]MFM uptake was shown to be linear for both cMATE2K and hMATE2K during the first 2 min (Fig. 2C). Mock-HEK cells transported substantially low quantities of MFM compared with the transporter-expressing cells, showing a non-saturable and linear uptake (Fig 2). A 2-min uptake window was selected for use in subsequent pH-dependent, kinetic and inhibition studies as it covered the initial rate of MFM uptake into the transporter-expressing cells.

MATE1- and MATE2K-mediated transport is stimulated by an oppositely directed proton gradient (Otsuka et al., 2005, Masuda et al., 2006, Konig et al., 2011). Therefore, specific uptake of 2 μM [^{14}C]MFM into the monkey transporter-expressing cells was measured in the presence of different extracellular pH conditions (5.0, 6.0, 7.0, 7.4, 8.0, 9.0, 10.0, and 11.0) (Fig. 3). The pH-dependence experiments have been done with the buffer containing HEPES. HEPES has a pKa of 7.5 at 25°C and provides robust buffering capacity in the pH range of 6.8 to 8.2. Although HEPES and HCL or NaOH can be blended to produce a buffer at any pH between 5 and 11 in the experiment, the buffering capacity may not be very good at pH beyond the range of 6.8 to 8.2. In the presence of stably-transfected HEK cells, cMATE1- and hMATE1-mediated MFM uptake was comparable at various extracellular pH values. Both cMATE1- and hMATE1-mediated uptake was increased with increasing extracellular pH and was maximal at pH 9.0, and then decreased when pH was raised from 9.0 to 11.0 (Fig. 3B). The cMATE2K- and hMATE2K-

DMD Fast Forward. Published on November 25, 2015 as DOI: 10.1124/dmd.115.066852
This article has not been copyedited and formatted. The final version may differ from this version.

mediated MFM uptake also demonstrated pH dependence. At low extracellular pH (less than 7.4), the MFM uptake is negligible, whereas the uptake increased significantly when pH was raised from pH 7.4 with maximum uptake at pH 10.0 (Fig. 3C). In contrast, cOCT2- and hOCT2-mediated uptake appeared considerably less sensitive to the increase of pH (less than 2.5-fold difference) (Fig. 3A). This observation is consistent with that reported in the literature (Urakami et al., 1998, Okuda et al., 1999). The assessment of pH-dependence of transport includes the measurement of [^{14}C]MFM uptake at high pH values that are physiologically irrelevant (greater than 8.0).

cOCT2, cMATE1, and cMATE2K Show Similar MFM Transport Kinetics as Compared to Human Organic Cation Transporters. To evaluate MFM transport kinetics by monkey and human organic cation transporters and compare the efficacy of transport and affinity for the substrate, the initial rates of MFM uptake, measured after 2 min incubation, were determined for MFM concentrations ranging from 4.6 to 10,000 μM. The uptake into transporter-overexpressing cells was corrected for nonspecific binding and passive diffusion components (i.e., uptake into mock-HEK cells at each concentration), as described under *Materials and Methods,* to obtain the saturable component (Fig. 4, open triangles and circles). All 3 cynomolgus monkey organic transporters showed similar saturable transport kinetics and followed a Michaelis-Menten curve for MFM uptake in comparison with the corresponding human transporters, with K_t and V_{max} less than 2.3-fold difference and only slight differences in CL_{int} values when normalized to total protein concentration in cell lysates (Table 2). To be specific, cMATE1 and hMATE1 showed the highest affinity for MFM among transporters in each species, with an estimated K_t of 340 ± 29.4 vs. 228 ± 15.3 μM, respectively, followed by OCT2 and MATE2K. Moreover, cOCT2 and hOCT2 showed the highest efficiency of transport,

DMD Fast Forward. Published on November 25, 2015 as DOI: 10.1124/dmd.115.066852
This article has not been copyedited and formatted. The final version may differ from this version.

with a CL_{int} of 105 vs. 104 μL/min/mg protein, that is, 6- to 12-fold higher than MATE1 and MATE2-K, which showed the same transport efficiency (17.4 vs. 19.7 and 10.2 vs. 8.7 μL/min/mg protein, respectively). Furthermore, when normalized to the expression of the individual transporter protein in each cell line, the monkey-to-human ratios of V_{max} and CL_{int} are less than 2-fold (Table 2). It should be noted that the V_{max}/K_t ratio (CL_{int}) determined for each transporter, employing the full range of substrate concentrations chosen, could be estimated based on the initial uptake rate measured at the low substrate concentration of 2 μM ($<< K_t$) (cOCT2: 44.2 vs. 105; hOCT2: 51.0 vs. 104; cMATE1: 17.2 vs. 17.4; hMATE1: 15.3 vs. 19.7; cMATE2K: 12.0 vs. 10.2; and hMATE2K: 6.0 vs. 8.7 μL/min per mg protein). Therefore, it is assumed that uptake rates across the range of substrate concentrations were linear with time.

PYR, CMD, QD, VDN, KCZ, and IPM inhibit cOCT2-, cMATE1-, and cMATE2K-Mediated MFM Uptake at Similar Concentrations as Compared to Human Organic Cation Transporters. To characterize species difference in inhibitory potencies of the standard organic cation inhibitors, a concentration-dependent effect of these compounds was evaluated in the transporter-overexpressing HEK 293 cells, and the concentrations of inhibitors rendering 50% inhibition of MFM uptake (IC_{50}) were evaluated by fitting the data as described under *Materials and Methods*. PYR, a known organic cation transporter inhibitor, equally inhibited MFM uptake by monkey and human transporters in a concentration-dependent manner (Fig. 5 and Table 3), with similar IC_{50} values observed for OCT2 (cOCT2 vs. hOCT2: 1.2 ± 0.38 vs. 4.1 ± 0.58 μM), MATE1 (cMATE1 vs. hMATE1: 0.17 ± 0.04 vs. 0.11 ± 0.04 μM), and MATE2K (cMATE2K vs. hMATE2K: 0.25 ± 0.04 vs. 0.15 ± 0.01 μM) (Table 3). This was also observed for other known inhibitors, with the exception of IPM against OCT2 (monkey vs. human: 12.3 ± 1.8 vs. 2.1 ± 0.10 μM) (Table 3; Supplemental Fig. 3). In all cases, because the MFM concentrations

DMD Fast Forward. Published on November 25, 2015 as DOI: 10.1124/dmd.115.066852
This article has not been copyedited and formatted. The final version may differ from this version.

used to generate the IC_{50}s were significantly lower than the K_t for monkey and human OCT2, MATE1, and MATE2K, the K_i values are likely equal to IC_{50} values if the transport inhibition is competitive in nature.

Effect of Intravenous (IV) PYR on the Pharmacokinetics of MFM. To examine the in vivo inhibitory effect of PYR on the MFM uptake mediated by renal organic cation transporters, a single IV dose DDI study was conducted with 3 male cynomolgus monkeys. The IV dose of PYR (0.5 mg/kg) increased the area under the concentration-time curve from time zero to infinity ($AUC_{0\text{-inf}}$) of IV MFM (Fig. 6A). The $AUC_{0\text{-inf}}$ of MFM was significantly increased by 123% (46.4 ± 9.0 vs. 102 ± 2.3 μM•hr) ($p < 0.01$); the 90% CI of the MFM AUC ratio was 1.57 to 3.17 (Table 4). There was a significant 54% (± 9%) decrease in MFM clearance (CL) ($p < 0.05$) and no change in steady-state volume of distribution (V_{ss}) between treatments (0.98 ± 0.16 vs. 0.88 ± 0.21 L/kg), resulting in a significant 98% increase in apparent terminal half-life ($T_{1/2}$) between treatments (7.1 ± 1.3 vs. 13.9 ± 1.8 hr) ($p < 0.01$). In addition, the monkey urine samples were collected for up to 48 hr following IV administration of MFM, and approximately 80% of the dose was excreted in the urine within 7 hr irrespective of PYR treatment (Fig. 7A). The decrease in total CL can be solely attributed to the decrease in renal clearance of MFM (CL_R) when co-administered with PYR (from 11.2 ± 2.4 to 5.0 ± 0.1 mL/min/kg vs. from 10.7 ± 3.1 to 5.3 mL/min/kg) (Table 4). Consistently almost complete MFM dose was excreted unchanged in the urine after IV administration with or without PYR (Fig. 7A).

The pharmacokinetics of PYR in monkeys was evaluated also. At a 15-min IV infusion dose of 0.5 mg/kg, the PYR plasma concentration at 1.25 hr post dose ($C_{1.5\ hr}$) was 571 ± 23.6 nM. The PYR plasma level at 49 hr after PYR dosing ($C_{49\ hr}$) was 82.9 ± 22.0 nM (Fig. 6C and Table 4).

Effect of PYR on the Pharmacokinetics of Oral MFM. It was also possible to conduct a single dose DDI study following an MFM oral dose of 8.6 mg/kg and an oral 2.5 mg/kg dose of PYR (2 male cynomolgus monkeys). The $AUC_{0\text{-inf}}$ of MFM decreased by 54% with concomitant PYR compared with MFM alone (65.7 vs. 30.6 μM•hr) (Fig. 6B; Table 5). Furthermore, the urinary recovery over the 0-24 hr collection period also reduced by 42% (Fig. 7B). As a result, there is no difference in CL_R between treatments (9.3 vs. 11.2 mL/min/kg) (Table 5). Following an oral dose of 2.5 mg/kg, PYR plasma levels reached a peak of 246 nM, with a T_{max} of 4.0 hr (Fig. 6C). PYR systemic exposure after the oral dose of 2.5 mg/kg was significantly less than after the IV dose of 0.5 mg/kg (Fig. 6C). For PYR, a second peak plasma concentration was apparent after IV and oral administration (Fig. 6C). Because enterohepatic recirculation of PYR has been demonstrated in rat, dog, and human (Cavallito et al., 1978, Coleman et al., 1985), it is hypothesized that the same process is operative in the monkey.

Discussion

Recently, an increasing number of investigators have utilized the cynomolgus monkey as a model to study the inhibition of drug transporters in vivo (Tahara et al., 2006, Shen et al., 2013, Takahashi et al., 2013, Uchida et al., 2014, Chu et al., 2015, Karibe et al., 2015, Shen et al., 2015b). Such a model offers advantages in drug development, when the transporter inhibition potential of a clinical candidate requires more extensive evaluation of changes in victim drug pharmacokinetics and organ toxicity. However, when compared to other transporters, there is very limited information related to cOCT2, cMATE1 and cMATE2K. All three are known to be expressed in the kidney and, like their human counterparts, likely function to mediated the secretion of substrates such as MFM, creatinine and cisplatin (Urakami et al., 2004, Tanihara et al., 2007, Tanihara et al., 2009, Imamura et al., 2011, Shen et al., 2015a). It is worth noting that although the impact of transporters on systemic exposure is relatively modest (less than 3-fold), their effects on drug distribution or tissue exposure could be more dramatic.

For the first time, the cloning of full-length cOCT2, cMATE1, and cMATE2K cDNAs is reported. The 3 cDNAs were shown to have a high derived amino acid sequence homology to hOCT2, hMATE1, and hMATE2K (96.9%, 96.0% and 97.4%, respectively) (Supplemental Fig. 1). It is notable that the counterparts of hMATE2K have not been cloned in rodents (Terada and Inui, 2008, Motohashi and Inui, 2013), and rabbit MATE2K has only 74% amino acid identity to hMATE2K (Zhang et al., 2007), although both hMATE1 and hMATE2K are highly expressed in kidney at similar mRNA levels. Two spliced isoforms of cMATE2K were identified that differ from each other by 15 residues. However, no human equivalent spliced deletion isoform has been reported. It is unknown which isoform represents the true wild-type, because cDNAs

representing each form were derived from a pooled kidney RNA prepared from 3 animals, and the frequency of these forms in a larger population was not determined. However, the deleted isoform unlikely encoded functional transporter since no increased activity was observed (versus mock cells) with [^{3}H]MPP^{+} and [^{14}C]MFM as substrates (Supplemental Fig. 2).

Functionally, monkey and human renal organic cation transporters were found to be very similar. For example, cOCT2, cMATE1, and cMATE2K transported MFM, MPP^{+}, TEA, and CMD into the transporter-overexpressing cells at similar rates comparable to hOCT2, hMATE1, and hMATE2K. In contrast, E3S and MTX, two organic anions, are unlikely substrates for monkey and human organic cation transporters, with the exception of E3S for hMATE2K (approximately 2-fold increased uptake into cMATE2K-HEK cells compared to Mock-HEK cells (Fig. 1). In addition, monkey and human renal organic transporters transported MFM into HEK 293 cells in similar time- and concentration-dependent manner (Figs. 2 and 4), resulting in a comparable K_t between two species (Table 2). The K_t values generated in the present studies are in agreement with those of human organic transporters reported previously (Kimura et al., 2005, Masuda et al., 2006, Choi et al., 2007, Tanihara et al., 2007, Chen et al., 2009, Zolk et al., 2009b, Zolk et al., 2009a, Meyer zu Schwabedissen et al., 2010). Moreover, the monkey-to-human ratios of V_{max} and CL_{int} are less than 2-fold when normalized to the individual transporter protein level in each cell line (Table 2), suggesting a similar transport rate and efficiency for OCT2, MATE1, and MATE2K between species. It has been reported that both hMATE1 and hMATE2K act as proton/substrate antiporters (Otsuka et al., 2005, Masuda et al., 2006, Muller et al., 2011), and we found that both cMATE1- and cMATE2K-mediated MFM transport were stimulated by an oppositely directed proton gradient with maximal uptake occurring at pH 9.0

and 10.0, respectively (Fig. 3). These results support the hypothesis that the transport functions of hOCT2, hMATE1, and hMATE2K are similar to those of the corresponding monkey forms.

Although several compounds (PYR, CMD, QD, VDN, KCZ, and IPM) were tested as inhibitors of MFM uptake by cOCT2, cMATE1, and cMATE2K in vitro (Table 3), PYR was selected for in vivo evaluation as an inhibitor, because it is a well-established potent inhibitor of MATE1- and MATE2K (Ito et al., 2010, Kusuhara et al., 2011). In 8 healthy volunteers, the concomitant oral administration of 50 mg PYR (as antimalarial) is known to inhibit renal MFM clearance by 23 and 35% at the microdose (100 μg) and therapeutic dose (250 mg), respectively, and increase MFM plasma *AUC* by 39% at the therapeutic dose but not following a microdose (Kusuhara et al., 2011). The interaction is likely the result of the inhibition of both basolateral OCT2 and apical MATEs. The plasma concentrations of PYR after a single oral dose of 50 mg PYR were not reported in the clinical study, and it was not possible to compare the total and unbound plasma drug levels to its IC_{50} values. In the present study, IV infusion of 0.5 mg/kg PYR in cynomolgus monkeys reduced MFM clearance by 54 ± 9%, resulting in an increase in MFM *AUC* by 123% (Table 4). This is in line with the in vivo inhibitory effect of PYR in humans (Kusuhara et al., 2011). In contrast, an IV infusion of 2 μmol/kg (or approximately 0.5 mg/kg) PYR in mice has been shown not to affect MFM plasma concentrations and urinary excretion rates, although the PYR pretreatment significantly increases the kidney-to-plasma ratios of MFM (Ito et al., 2010).

In the present study, oral co-administration of 2.5 mg/kg PYR to cynomolgus monkeys decreased MFM *AUC* by 54% (Table 5). Such a decrease in MFM AUC appears to contradict PYR's potent inhibition of the luminal efflux (Tables 3 and Fig. 5). This discrepancy can be explained as follows. First, the blood and renal proximal tubular intracellular concentrations of

PYR after oral administration are unlikely sufficient to affect the vectorial transport of MFM across renal proximal tubules. This view is supported by the fact that the CL_R of MFM was not changed at all after oral treatment of PYR (Table 5). Indeed, the C_{max} and *AUC* values in monkeys after oral administration of 2.5 mg/kg PYR are estimated to be 7- and 41-fold less than those in humans when dosed orally at 50 mg (Weidekamm et al., 1982), and approximately 3-fold less than those in monkeys after IV dose of 0.5 mg/kg PYR (Tables 4 and 5). The absolute oral bioavailability (F) of PYR in monkeys is approximately 7%, which is less than that reported for human subjects (~ 17%) (Weidekamm et al., 1982, Karibe et al., 2015). Given the fact that IV *CL* of PYR is low compared to monkey hepatic blood flow (2.4 versus 44 mL/min/kg), liver extraction cannot explain the low plasma levels after PYR oral administration. For PYR, therefore, incomplete absorption and gut first pass is implicated. One or both can render a lower $C_{max,u}/IC_{50}$ ratio following a PO dose. As described above, consistent with reports employing hOCT2, hMATE1, and hMATE2K (Takano et al., 1984, Ito et al., 2010, Kusuhara et al., 2011), PYR was shown to be an cOCT2, cMATE1, and cMATE2K inhibitor with IC_{50} values of 1.2 ± 0.38, 0.17 ± 0.04, and 0.25 ± 0.04 μM, respectively (Table 3). Assuming that the binding of PYR to monkey plasma proteins is equal to that of human plasma proteins (i.e. 94%) (Hsyu and Giacomini, 1987), the $C_{max,u}/IC_{50}$ ratios after IV infusion of 0.5 mg/kg PYR are greater than the cutoff level of 0.1 for renal transporter inhibition (0.03, 0.21, and 0.15 for cOCT2, cMATE1 and cMATE2K, respectively), necessitating the conduct of a clinical DDI study based on the proposed US Food and Drug Administration (FDA) guidelines (US FDA, 2012). Furthermore, the $C_{max,u}/IC_{50}$ ratios after oral administration of 2.5 mg/kg PYR are less than the cutoff level (0.01, 0.09 and 0.06 for cOCT2, cMATE1 and cMATE2K, respectively).

Second, it is hypothesized that oral treatment of PYR affects MFM absorption in cynomolgus monkeys. MFM is hydrophilic base that exists as a cationic species under physiological pH conditions and has poor passive membrane permeability. The intestinal absorption of MFM is incomplete and dose-dependent (bioavailability of 86 to 42% as the dose increases from 0.25 to 2.0 g), and it has been suggested that MFM absorption is mediated by an active, saturable absorption process (Scheen, 1996, Bell and Hadden, 1997, Klepser and Kelly, 1997). In this study, the F values in monkeys after oral administration of 8.6 mg/kg MFM in the absence and presence of PYR are estimated to be 64% and 30%, respectively. Consistently, the accumulative urinary excretion of MFM dose over 24 hr in the absence and presence of PYR are 65.7% and 30.6%, respectively (Table 5; Fig. 7). However, the transporters mediating active uptake MFM in the intestine have not been well defined; OCT3 (Muller et al., 2005, Wright, 2005), plasma membrane monoamine transporter (Zhou et al., 2007), and OCTN1 (Nakamichi et al., 2013) have been implicated. Therefore, additional studies may be warranted in order to more comprehensively evaluate the transporters governing the disposition of MFM in monkeys and humans.

In summary, based on the results of the present study, it is concluded that the cynomolgus monkey may serve as a surrogate animal model to more accurately assess pharmacokinetic changes and toxicity potential occurring as a result of DDIs involving inhibition of renal OCT2, MATE1, and MATE2K.

Acknowledgments

The authors wish to thank Sanjith Kallipatti and Sabariya Selvam (Bristol-Myers Squibb Biocon R&D Center, Bangalore, India) for designing cloning primers for cynomolgus monkey OCT2, MATE1, and MATE2K. We also thank Sumit Gupta for synthesizing cDNA from cynomolgus monkey kidney RNA.

Authorship Contributions

Participated in research design: Shen, Mintier, Fancher, Zeng, Rodrigues, Marathe, and Lai

Conducted experiments: Shen, Liu, Jiang, Titsch, Taylor, Qiu, Chen, Sukrutharaj, Kuit, Mintier, and Krishnamurthy.

Contributed new reagents or analytic tools: Shen, Liu, Jiang, Titsch, and Mintier.

Performed data analysis: Shen, Liu, Jiang, Kandoussi, Mintier, and Lai.

Wrote or contributed to the writing of the manuscript: Shen, Jiang, Qiu, Mintier, Rodrigues, Marathe, and Lai.

References

Alnouti Y, Petrick JS and Klaassen CD (2006) Tissue distribution and ontogeny of organic cation transporters in mice. *Drug Metab Dispos* 34: 477-482.

Bell PM and Hadden DR (1997) Metformin. *Endocrinol Metab Clin North Am* 26: 523-537.

Bleasby K, Castle JC, Roberts CJ, Cheng C, Bailey WJ, Sina JF, Kulkarni AV, Hafey MJ, Evers R, Johnson JM, Ulrich RG and Slatter JG (2006) Expression profiles of 50 xenobiotic transporter genes in humans and pre-clinical species: a resource for investigations into drug disposition. *Xenobiotica* 36: 963-988.

Cavallito JC, Nichol CA, Brenckman WD, Jr., Deangelis RL, Stickney DR, Simmons WS and Sigel CW (1978) Lipid-soluble inhibitors of dihydrofolate reductase. I. Kinetics, tissue distribution, and extent of metabolism of pyrimethamine, metoprine, and etoprine in the rat, dog, and man. *Drug Metab Dispos* 6: 329-337.

Chen Y, Teranishi K, Li S, Yee SW, Hesselson S, Stryke D, Johns SJ, Ferrin TE, Kwok P and Giacomini KM (2009) Genetic variants in multidrug and toxic compound extrusion-1, hMATE1, alter transport function. *Pharmacogenomics J* 9: 127-136.

Choi MK, Jin QR, Jin HE, Shim CK, Cho DY, Shin JG and Song IS (2007) Effects of tetraalkylammonium compounds with different affinities for organic cation transporters on the pharmacokinetics of metformin. *Biopharm Drug Dispos* 28: 501-510.

Chu X, Shih SJ, Shaw R, Hentze H, Chan GH, Owens K, Wang S, Cai X, Newton D, Castro-Perez J, Salituro G, Palamanda J, Fernandis A, Ng CK, Liaw A, Savage MJ and Evers R (2015) Evaluation of cynomolgus monkeys for the identification of endogenous biomarkers for hepatic transporter inhibition and as a translatable model to predict pharmacokinetic interactions with statins in humans. *Drug Metab Dispos* 43: 851-863.

Coleman MD, Mihaly GW, Edwards G, Ward SA, Howells RE and Breckenridge AM (1985) Pyrimethamine pharmacokinetics and its tissue localization in mice: effect of dose size. *J Pharm Pharmacol* 37: 170-174.

European Medicines Agency (EMA), Science Medicines Health, Committee for Human Medicinal Products (CHMP). Guideline on the Investigation of Drug Interactions. *EMA website http://www.ema.europa.eu/docs/en_GB/document_library/Scientific_guideline/2012/07/WC500129606.pdf,* (2012)

Fisel P, Renner O, Nies AT, Schwab M and Schaeffeler E (2014) Solute carrier transporter and drug-related nephrotoxicity: the impact of proximal tubule cell models for preclinical research. *Expert Opin Drug Metab Toxicol* 10: 395-408.

Hsyu PH and Giacomini KM (1987) The pH gradient-dependent transport of organic cations in the renal brush border membrane. Studies with acridine orange. *J Biol Chem* 262: 3964-3968.

Imamura Y, Murayama N, Okudaira N, Kurihara A, Okazaki O, Izumi T, Inoue K, Yuasa H, Kusuhara H and Sugiyama Y (2011) Prediction of fluoroquinolone-induced elevation in serum creatinine levels: a case of drug-endogenous substance interaction involving the inhibition of renal secretion. *Clin Pharmacol Ther* 89: 81-88.

International Transporter C, Giacomini KM, Huang SM, Tweedie DJ, Benet LZ, Brouwer KL, Chu X, Dahlin A, Evers R, Fischer V, Hillgren KM, Hoffmaster KA, Ishikawa T, Keppler D, Kim RB, Lee CA, Niemi M, Polli JW, Sugiyama Y, Swaan PW, Ware JA, Wright SH, Yee SW, Zamek-Gliszczynski MJ and Zhang L (2010) Membrane transporters in drug development. *Nat Rev Drug Discov* 9: 215-236.

Ito S, Kusuhara H, Kuroiwa Y, Wu C, Moriyama Y, Inoue K, Kondo T, Yuasa H, Nakayama H, Horita S and Sugiyama Y (2010) Potent and specific inhibition of mMate1-mediated efflux of type I organic cations in the liver and kidney by pyrimethamine. *J Pharmacol Exp Ther* 333: 341-350.

Jaiswal S, Sharma A, Shukla M, Vaghasiya K, Rangaraj N and Lal J (2014) Novel pre-clinical methodologies for pharmacokinetic drug-drug interaction studies: spotlight on "humanized" animal models. *Drug Metab Rev* 46: 475-493.

Karibe T, Hagihara-Nakagomi R, Abe K, Imaoka T, Mikkaichi T, Yasuda S, Hirouchi M, Watanabe N, Okudaira N and Izumi T (2015) Evaluation of the usefulness of breast cancer resistance protein (BCRP) knockout mice and BCRP inhibitor-treated monkeys to estimate the clinical impact of BCRP modulation on the pharmacokinetics of BCRP substrates. *Pharm Res* 32: 1634-1647.

Kimura N, Masuda S, Tanihara Y, Ueo H, Okuda M, Katsura T and Inui K (2005) Metformin is a superior substrate for renal organic cation transporter OCT2 rather than hepatic OCT1. *Drug Metab Pharmacokinet* 20: 379-386.

Klepser TB and Kelly MW (1997) Metformin hydrochloride: an antihyperglycemic agent. *Am J Health Syst Pharm* 54: 893-903.

Konig J, Zolk O, Singer K, Hoffmann C and Fromm MF (2011) Double-transfected MDCK cells expressing human OCT1/MATE1 or OCT2/MATE1: determinants of uptake and transcellular translocation of organic cations. *Br J Pharmacol* 163: 546-555.

Kusuhara H, Ito S, Kumagai Y, Jiang M, Shiroshita T, Moriyama Y, Inoue K, Yuasa H and Sugiyama Y (2011) Effects of a MATE protein inhibitor, pyrimethamine, on the renal

elimination of metformin at oral microdose and at therapeutic dose in healthy subjects. *Clin Pharmacol Ther* 89: 837-844.

Masuda S, Terada T, Yonezawa A, Tanihara Y, Kishimoto K, Katsura T, Ogawa O and Inui K (2006) Identification and functional characterization of a new human kidney-specific H+/organic cation antiporter, kidney-specific multidrug and toxin extrusion 2. *J Am Soc Nephrol* 17: 2127-2135.

Meyer zu Schwabedissen HE, Verstuyft C, Kroemer HK, Becquemont L and Kim RB (2010) Human multidrug and toxin extrusion 1 (MATE1/SLC47A1) transporter: functional characterization, interaction with OCT2 (SLC22A2), and single nucleotide polymorphisms. *Am J Physiol Renal Physiol* 298: F997-F1005.

Morrissey KM, Stocker SL, Wittwer MB, Xu L and Giacomini KM (2013) Renal transporters in drug development. *Annu Rev Pharmacol Toxicol* 53: 503-529.

Motohashi H and Inui K (2013) Multidrug and toxin extrusion family SLC47: physiological, pharmacokinetic and toxicokinetic importance of MATE1 and MATE2-K. *Mol Aspects Med* 34: 661-668.

Motohashi H, Nakao Y, Masuda S, Katsura T, Kamba T, Ogawa O and Inui K (2013) Precise comparison of protein localization among OCT, OAT, and MATE in human kidney. *J Pharm Sci* 102: 3302-3308.

Motohashi H, Sakurai Y, Saito H, Masuda S, Urakami Y, Goto M, Fukatsu A, Ogawa O and Inui K (2002) Gene expression levels and immunolocalization of organic ion transporters in the human kidney. *J Am Soc Nephrol* 13: 866-874.

Muller F, Konig J, Glaeser H, Schmidt I, Zolk O, Fromm MF and Maas R (2011) Molecular mechanism of renal tubular secretion of the antimalarial drug chloroquine. *Antimicrob Agents Chemother* 55: 3091-3098.

Muller J, Lips KS, Metzner L, Neubert RH, Koepsell H and Brandsch M (2005) Drug specificity and intestinal membrane localization of human organic cation transporters (OCT). *Biochem Pharmacol* 70: 1851-1860.

Nakamichi N, Shima H, Asano S, Ishimoto T, Sugiura T, Matsubara K, Kusuhara H, Sugiyama Y, Sai Y, Miyamoto K, Tsuji A and Kato Y (2013) Involvement of carnitine/organic cation transporter OCTN1/SLC22A4 in gastrointestinal absorption of metformin. *J Pharm Sci* 102: 3407-3417.

Okuda M, Saito H, Urakami Y, Takano M and Inui K (1996) cDNA cloning and functional expression of a novel rat kidney organic cation transporter, OCT2. *Biochem Biophys Res Commun* 224: 500-507.

Okuda M, Urakami Y, Saito H and Inui K (1999) Molecular mechanisms of organic cation transport in OCT2-expressing Xenopus oocytes. *Biochim Biophys Acta* 1417: 224-231.

Otsuka M, Matsumoto T, Morimoto R, Arioka S, Omote H and Moriyama Y (2005) A human transporter protein that mediates the final excretion step for toxic organic cations. *Proc Natl Acad Sci U S A* 102: 17923-17928.

Qiu X, Bi YA, Balogh LM and Lai Y (2013) Absolute measurement of species differences in sodium taurocholate cotransporting polypeptide (NTCP/Ntcp) and its modulation in cultured hepatocytes. *J Pharm Sci* 102: 3252-3263.

Scheen AJ (1996) Clinical pharmacokinetics of metformin. *Clin Pharmacokinet* 30: 359-371.

Shen H, Liu T, Morse BL, Zhao Y, Zhang Y, Qiu X, Chen C, Lewin AC, Wang XT, Liu G, Christopher LJ, Marathe P and Lai Y (2015a) Characterization of Organic Anion Transporter 2 (SLC22A7): A Highly Efficient Transporter for Creatinine and Species-Dependent Renal Tubular Expression. *Drug Metab Dispos* 43: 984-993.

Shen H, Su H, Liu T, Yao M, Mintier G, Li L, Fancher RM, Iyer R, Marathe P, Lai Y and Rodrigues AD (2015b) Evaluation of rosuvastatin as an organic anion transporting polypeptide (OATP) probe substrate: in vitro transport and in vivo disposition in cynomolgus monkeys. *J Pharmacol Exp Ther* 353: 380-391.

Shen H, Yang Z, Mintier G, Han YH, Chen C, Balimane P, Jemal M, Zhao W, Zhang R, Kallipatti S, Selvam S, Sukrutharaj S, Krishnamurthy P, Marathe P and Rodrigues AD (2013) Cynomolgus monkey as a potential model to assess drug interactions involving hepatic organic anion transporting polypeptides: in vitro, in vivo, and in vitro-to-in vivo extrapolation. *J Pharmacol Exp Ther* 344: 673-685.

Tahara H, Kusuhara H, Chida M, Fuse E and Sugiyama Y (2006) Is the monkey an appropriate animal model to examine drug-drug interactions involving renal clearance? Effect of probenecid on the renal elimination of H2 receptor antagonists. *J Pharmacol Exp Ther* 316: 1187-1194.

Tahara H, Kusuhara H, Endou H, Koepsell H, Imaoka T, Fuse E and Sugiyama Y (2005) A species difference in the transport activities of H2 receptor antagonists by rat and human renal organic anion and cation transporters. *J Pharmacol Exp Ther* 315: 337-345.

Takahashi T, Ohtsuka T, Yoshikawa T, Tatekawa I, Uno Y, Utoh M, Yamazaki H and Kume T (2013) Pitavastatin as an in vivo probe for studying hepatic organic anion transporting

polypeptide-mediated drug-drug interactions in cynomolgus monkeys. *Drug Metab Dispos* 41: 1875-1882.

Takano M, Inui K, Okano T, Saito H and Hori R (1984) Carrier-mediated transport systems of tetraethylammonium in rat renal brush-border and basolateral membrane vesicles. *Biochim Biophys Acta* 773: 113-124.

Tang C and Prueksaritanont T (2010) Use of in vivo animal models to assess pharmacokinetic drug-drug interactions. *Pharm Res* 27: 1772-1787.

Tanihara Y, Masuda S, Katsura T and Inui K (2009) Protective effect of concomitant administration of imatinib on cisplatin-induced nephrotoxicity focusing on renal organic cation transporter OCT2. *Biochem Pharmacol* 78: 1263-1271.

Tanihara Y, Masuda S, Sato T, Katsura T, Ogawa O and Inui K (2007) Substrate specificity of MATE1 and MATE2-K, human multidrug and toxin extrusions/H(+)-organic cation antiporters. *Biochem Pharmacol* 74: 359-371.

Terada T and Inui K (2008) Physiological and pharmacokinetic roles of H+/organic cation antiporters (MATE/SLC47A). *Biochem Pharmacol* 75: 1689-1696.

Uchida Y, Wakayama K, Ohtsuki S, Chiba M, Ohe T, Ishii Y and Terasaki T (2014) Blood-brain barrier pharmacoproteomics-based reconstruction of the in vivo brain distribution of P-glycoprotein substrates in cynomolgus monkeys. *J Pharmacol Exp Ther* 350: 578-588.

Urakami Y, Kimura N, Okuda M and Inui K (2004) Creatinine transport by basolateral organic cation transporter hOCT2 in the human kidney. *Pharm Res* 21: 976-981.

Urakami Y, Okuda M, Masuda S, Saito H and Inui KI (1998) Functional characteristics and membrane localization of rat multispecific organic cation transporters, OCT1 and OCT2, mediating tubular secretion of cationic drugs. *J Pharmacol Exp Ther* 287: 800-805.

US FDA. Guidance for Industry. Drug Interaction Studies — Study Design, Data Analysis, and Implications for Dosing and Labeling. *US FDA website http://www.fda.gov/downloads/Drugs/GuidanceComplianceRegulatoryInformation/Guidances/UCM292362.pdf*, (2012).

Weidekamm E, Plozza-Nottebrock H, Forgo I and Dubach UC (1982) Plasma concentrations in pyrimethamine and sulfadoxine and evaluation of pharmacokinetic data by computerized curve fitting. *Bull World Health Organ* 60: 115-122.

Wright SH (2005) Role of organic cation transporters in the renal handling of therapeutic agents and xenobiotics. *Toxicol Appl Pharmacol* 204: 309-319.

Zhang X, Cherrington NJ and Wright SH (2007) Molecular identification and functional characterization of rabbit MATE1 and MATE2-K. *Am J Physiol Renal Physiol* 293: F360-370.

Zhou M, Xia L and Wang J (2007) Metformin transport by a newly cloned proton-stimulated organic cation transporter (plasma membrane monoamine transporter) expressed in human intestine. *Drug Metab Dispos* 35: 1956-1962.

Zolk O, Solbach TF, Konig J and Fromm MF (2009a) Functional characterization of the human organic cation transporter 2 variant p.270Ala>Ser. *Drug Metab Dispos* 37: 1312-1318.

Zolk O, Solbach TF, Konig J and Fromm MF (2009b) Structural determinants of inhibitor interaction with the human organic cation transporter OCT2 (SLC22A2). *Naunyn Schmiedebergs Arch Pharmacol* 379: 337-348.

Footnotes

Reprint requests: Hong Shen, F1.3802, Route 206 & Province Line Road., Bristol-Myers Squibb Company, Princeton, NJ 08543. Telephone: (609) 252-4509; Facsimile: (609) 252-6802

This study is supported by Bristol-Myers Squibb Company.

Figure Legends

Fig. 1. Comparison of uptake of [^{14}C]MFM (A), [^{3}H]MPP^{+} (B), [^{14}C]TEA (C), [^{3}H]CMD, [^{3}H]E3S (E), and [^{3}H]MTX (F) into HEK 293 cells overexpressing cynomolgus monkey and human OCT2, MATE1, or MATE2K and into vector control cells (mock). Cells were incubated for 5 min with the radio-labeled compounds. Data are shown as mean ± SD (n = 3). * $p < 0.05$, ** $p < 0.01$, and ***$p < 0.001$, when the uptake with transporter-expressing cells was compared with that in mock cell.

Fig. 2. Time course for the uptake of [^{14}C]MFM into HEK 293 cells overexpressing cynomolgus monkey and human OCT2 (A), MATE1 (B), or MATE2K (C), as compared to vector control cells (mock). Cells were incubated with 2 μM [^{14}C]MFM up to 10 min. Data are shown as mean ± SD (n = 3).

Fig. 3. pH-dependent uptake of [^{14}C]MFM into HEK 293 cells overexpressing cynomolgus monkey and human OCT2 (A), MATE1 (B), or MATE2K (C). Cells were incubated with 1 μM [^{14}C]MFM for 2 min. Extracellular pH was varied between 5.0 and 11.0. Data are shown as mean ± SD (n = 3).

Fig. 4. Concentration-dependent uptake of [^{14}C]MFM into HEK 293 cells overexpressing cynomolgus monkey and human OCT2 (A), MATE1 (B), or MATE2K (C). Cells were incubated with [^{14}C]MFM (4.6 to 10,000 μM) for 2 min (linear range). Transporter-mediated [^{14}C]MFM transport was determined as the difference in uptake into the transporter overexpressing cells versus mock cells at each substrate concentration. The curves represent the best fit of the

Michaelis-Menten equation (mock subtracted net-active uptake component). Data are shown as mean ± SD (n = 3).

Fig. 5. Inhibition of OCT2- (A), MATE1- (B), and MATE2K-mediated uptake of [^{14}C]MFM (C) by PYR. Increasing concentrations of PYR (0.21 to150 μM for OCT2, 0.01 to 5.6 μM for MATEs) were added simultaneously with 2 μM [^{14}C]MFM for 2 min incubation (linear range). Extracellular pH was 7.4 or 8.4 for OCT2 or MATEs, respectively. The extent of inhibition of transporter-mediated uptake is expressed as a percentage of the uptake in the absence of inhibitor. Nonlinear regression analysis of the data was used to determine apparent IC_{50} values of PYR (IC_{50}s reported in Table 3). Data are shown as mean ± SD (n = 3).

Fig. 6. Mean plasma concentrations of MFM (A, IV dose; and B, oral dose) and PYR (C) in cynomolgus monkeys after a single intravenous dose of 3.9 mg/kg MFM with and without PYR given as an intravenous dose (0.5 mg/kg; n = 3) and after a single oral dose of 8.6 mg/kg MFM with and without PYR given as an oral dose (2.5 mg/kg; n = 2). Insets depict the same data over a 7-h period.

Fig. 7. Effects of PYR on urinary exertion of MFM after a single IV dose of MFM (3.9 mg/kg) alone or with PYR (0.5 mg/kg, IV) (A), and after single oral dose of MFM (8.6 mg/kg) alone or with PYR (2.5 mg/kg, PO) (B) in cynomolgus monkeys. The amount of MFM excreted in urine in monkeys was determined for the MFM alone (closed square) and PYR-treated (open square) groups. PYR was dosed one hour ahead of MFM.

Table 1

Summary of Proteo-specific Peptides and Their Respective MRM Transitions Used for Renal Organic Cation Transporter Protein Quantification with LC-MS/MS

			MRM Transition (*m/z*)[a]			
Protein	**Peptide**	**Mass (Da)**	**Q1**	**Q3.1**	**Q3.2**	**Q3.3**
OCT2	SLPASLQR	871	436	672	574	503
	SLPASLQ***R***[c]	881	441	682	584	513
MATE1[b]	GGPEATLEVR	1027	515	688	617	458
	GGPEATLEV***R***[c]	1037	520	698	627	463
MATE2K	YLQNQK	792	397	630	517	389
	YLQNQ***K***[c]	800	401	638	525	397

Table 1 Legend:

[a]Theoretical *m/z* value of doubly charged ions of intact peptide (Q1) assumed as precursor ions, and singly charged fragment ions derived from precursor ion indicated as Q3.1, Q3.2, and Q3.3.

[b]There is a difference of one amino acid in the MATE1 peptide between species (Human vs. monkey: GGPEATLEVR vs. GGPEATLELR). The expression level of cMATE1 was calculated by using human MATE1 standard.

[c]The labeling of Arg (R) or Lys (K) was done by introducing the stable isotope ([^{13}C] or [^{15}N]).

Table 2

Parameters Describing the Kinetics of MFM Transport by Cynomolgus Monkey and Human OCT2, MATE1, and MATE2K

Transporter	K_t µM	V_{max} nmol/min/mg protein	Cl_{int} µL/min/mg protein	V_{max} Ratio[a]	CL_{int} Ratio[a]
cOCT2	628 ± 66.2	66.0 ± 5.0	105	0.64	1.50
hOCT2	1,465 ± 165	153 ± 13.4	104		
cMATE1	340 ± 29.4	5.9 ± 0.34	17.4	1.24	0.84
hMATE1	228 ± 15.3	4.5 ± 0.19	19.7		
cMATE2K	1,566 ± 407	15.9 ± 1.8	10.2	1.00	0.52
hMATE2K	819 ± 69.5	7.1 ± 0.24	8.7		

Table 2 Legend:

Data are shown as mean ± SD (n = 3). The kinetic parameters were determined as indicated under *Materials and Methods*.

Intrinsic transport clearance (CL_{int}) was determined by dividing the V_{max} value by the K_t value

[a]Monkey-to-human V_{max} and CL_{int} ratios are normalized to the expression of individual transporter protein.

Table 3

Inhibition of Cynomolgus Monkey and Human Organic Cation Transporters by 6 Selected Inhibitors

	IC_{50} (μM)					
Compound	**cOCT2**	**hOCT2**	**cMATE1**	**hMATE1**	**cMATE2K**	**hMATE2K**
PYR	1.2 ± 0.38	4.1 ± 0.58	0.17 ± 0.04	0.11 ± 0.04	0.25 ± 0.04	0.15 ± 0.01
CMD	167 ± 15.1	200 ± 55.1	4.9 ± 1.0	2.3 ± 0.29	32.2 ± 4.2	13.5 ± 4.1
QD	19.4 ± 2.1	19.5 ± 2.1	22.0 ± 0.69	9.9 ± 1.2	18.5 ± 2.7	5.2 ± 1.1
VDN	3.3 ± 0.79	7.7 ± 1.0	1.4 ± 0.15	0.46 ± 0.12	0.45 ± 0.04	0.30 ± 0.02
KCZ	0.92 ± 0.17	1.6 ± 0.23	2.7 ± 0.41	1.1 ± 0.13	25.0 ± 3.6	23.5 ± 2.9
IPM	12.3 ± 1.8	2.1 ± 0.10	48.4 ± 5.8	37.5 ± 7.2	73.5 ± 11.6	76.0 ± 17.7

Legend to Table 3:

Data are shown as mean ± SD (n = 3). The IC_{50} values were determined as indicated under *Materials and Methods*. MFM (2 µM) was used as substrate. Therefore, the ratio of MFM concentration to K_t is very low (<0.01) and the reported IC_{50} values are considered estimates of K_i (assuming competitive inhibition).

Table 4

Summary of Pharmacokinetic Parameters for MFM and PYR in Cynomolgus Monkeys (n = 3) after a Single IV Dose of MFM (3.9 mg/kg) with and without an IV Dose of PYR (0.5 mg/kg)

Analyte	Variable	MFM Alone	With PYR	Ratio (90% CI)
MFM	**$AUC_{0\text{-}inf}$ (μM•hr)**	46.4 ± 9.0	102 ± 2.3**	2.23 (1.57-3.17)
	***Vss* (L/kg)**	0.98 ± 0.16	0.88 ± 0.21	0.88 (0.45-1.73)
	***CL* (mL/min/kg)**	11.2 ± 2.4	5.0 ± 0.1*	0.45 (0.32-0.64)
	% Urinary Excretion of Dose (0-48 hr)	94.1 ± 8.4	105 (79.8 and 130)[a]	NC
	CL_R (mL/min/kg)	10.7 ± 3.1	5.3 (3.9 and 6.7)[a]	NC
	$T_{1/2}$ (hr)	7.1 ± 1.3	13.9 ± 1.8**	1.98 (1.74-2.25)
PYR	**C_{max} (nM)**		607 ± 14.7	
	$AUC_{0\text{-}49hr}$ (nM•hr)		11,300 ± 983	
	***Vss* (L/kg)**		4.0 ± 0.6	
	***CL* (mL/min/kg)**		2.4 ± 0.3	
	$C_{49\ hr}$ (nM)		82.9 ± 22.0	
	$T_{1/2}$ (hr)		20.9 ± 5.2	

Table 4 Legend:

Data are shown as mean ± SD (n = 3 animals). The pharmacokinetic parameters were determined as indicated under *Materials and Methods*. PYR was intravenously dosed 60 min prior to MFM.

[a]Cage malfunction prevented urine collection from one animal in the co-administration treatment group (N = 2).

* $p < 0.05$ and ** $p < 0.01$ compared with values for the in the absence of PYR; NC, not calculated.

Table 5

Summary of Pharmacokinetic Parameters for MFM and PYR in Cynomolgus Monkeys (n = 2) after a Single Oral Dose of MFM (8.6 mg/kg) with and without an Oral PYR Dose (2.5 mg/kg)

Analyte	Variable	Animal #1		Animal #2		Average	
		MFM Alone	With PYR	MFM Alone	With PYR	MFM Alone	With PYR
MFM	C_{max} (µM)	11.4	4.8	21.3	7.8	16.4	6.3
	Tmax (hr)	2.0	3.0	0.8	2.0	1.4	2.5
	$AUC_{0\text{-}24hr}$ (µM•hr)	62.6	24.0	67.2	34.4	64.9	29.2
	$AUC_{0\text{-}inf}$ (µM•hr)	63.9	25.6	67.6	35.6	65.7	30.6
	% Urinary Excretion of Dose (0-24 hr)	57.9	25.5	50.8	37.0	54.5	30.8
	CL_R (mL/min/kg)	10.1	11.1	8.4	11.6	9.2	11.3
	$T_{1/2}$ (hr)	4.0	5.5	3.1	4.5	3.6	5.0
PYR	C_{max} (nM)		227		265		246
	Tmax (hr)		4.0		4.0		4.0
	$AUC_{0\text{-}25hr}$ (nM•hr)		3381		4033		3707
	$C_{25\ hr}$ (nM)		122		126		124
	$T_{1/2}$ (hr)		30.7		22.9		26.8

Legend to Table 5:

Data from individual animal are shown (n = 2 animals). The pharmacokinetic parameters were determined as indicated under *Materials and Methods*. PYR was orally dosed 60 min prior to MFM.

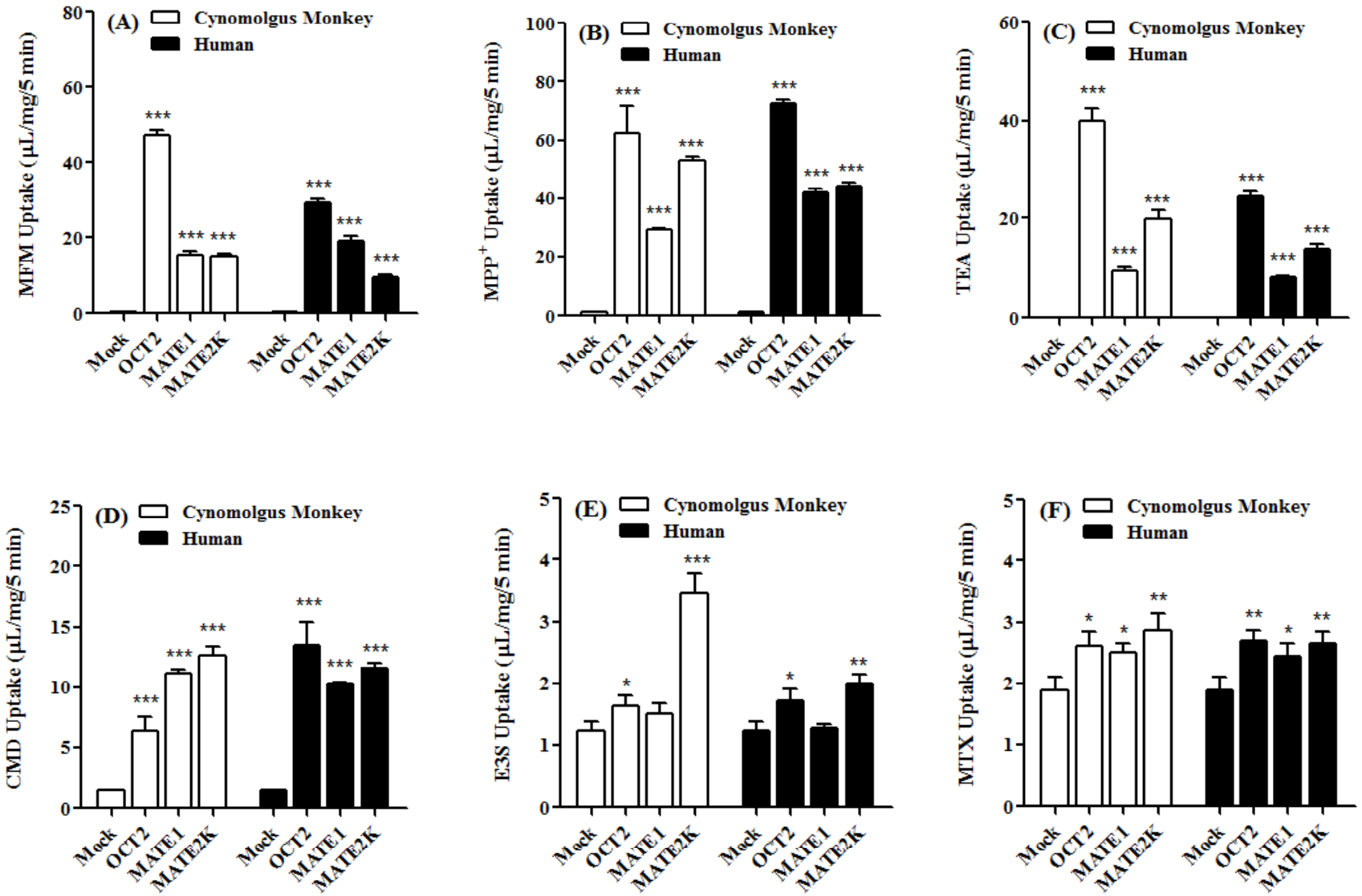

Figure 1

DMD Fast Forward. Published on November 25, 2015 as DOI: 10.1124/dmd.115.066852
This article has not been copyedited and formatted. The final version may differ from this version.

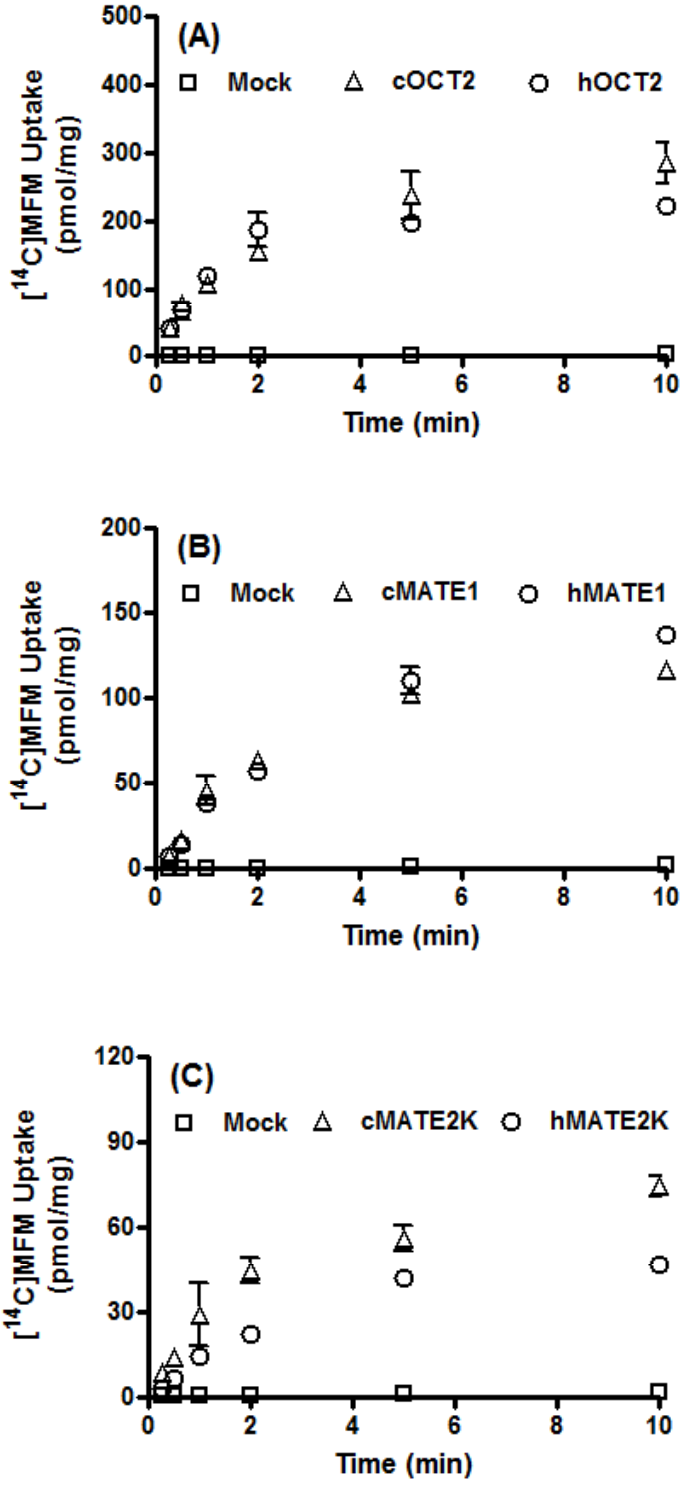

Figure 2

DMD Fast Forward. Published on November 25, 2015 as DOI: 10.1124/dmd.115.066852
This article has not been copyedited and formatted. The final version may differ from this version.

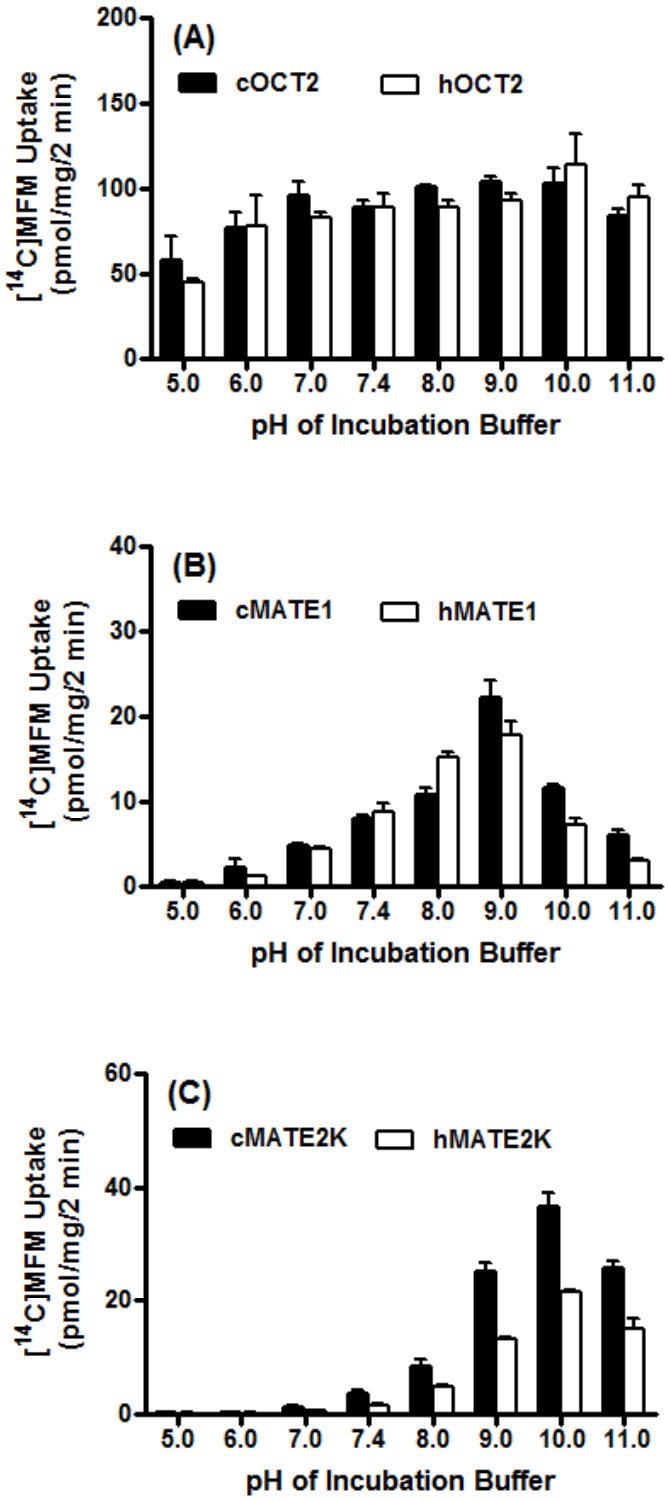

Figure 3

DMD Fast Forward. Published on November 25, 2015 as DOI: 10.1124/dmd.115.066852
This article has not been copyedited and formatted. The final version may differ from this version.

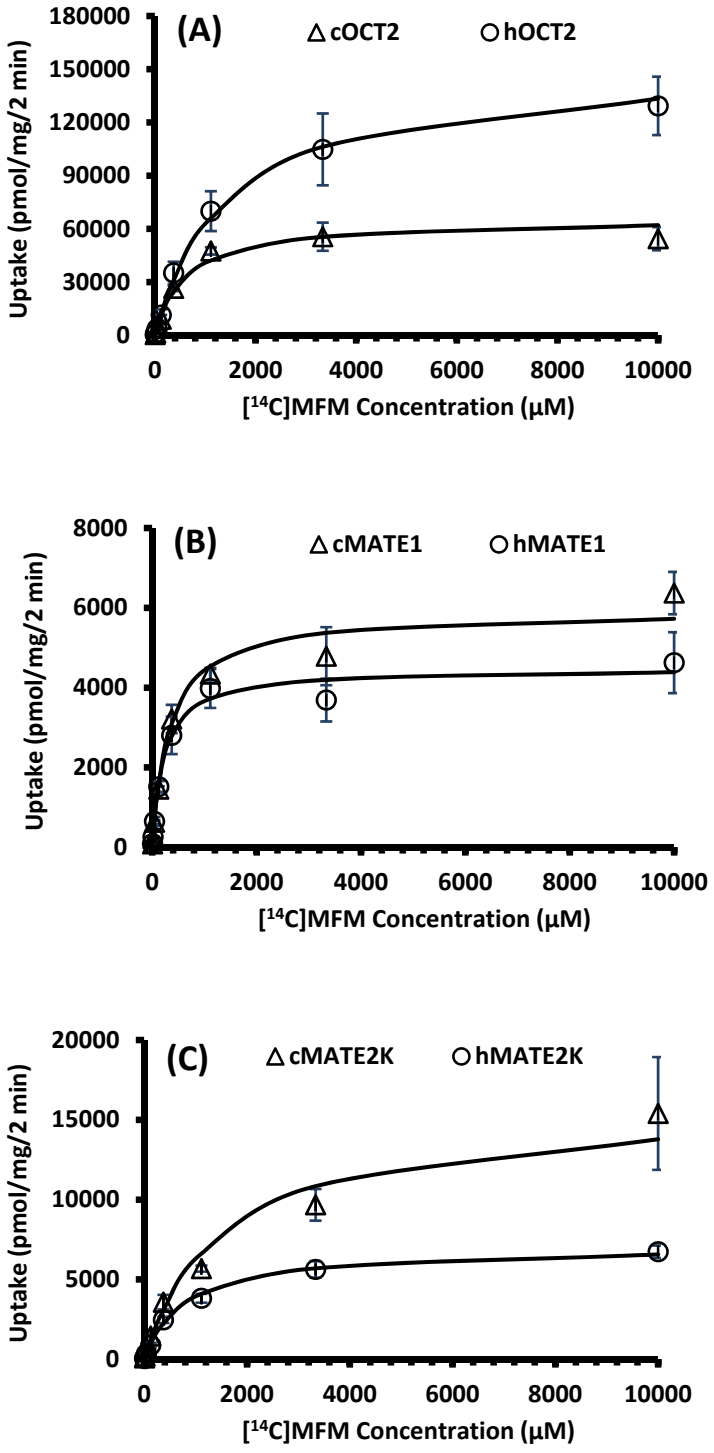

Figure 4

DMD Fast Forward. Published on November 25, 2015 as DOI: 10.1124/dmd.115.066852
This article has not been copyedited and formatted. The final version may differ from this version.

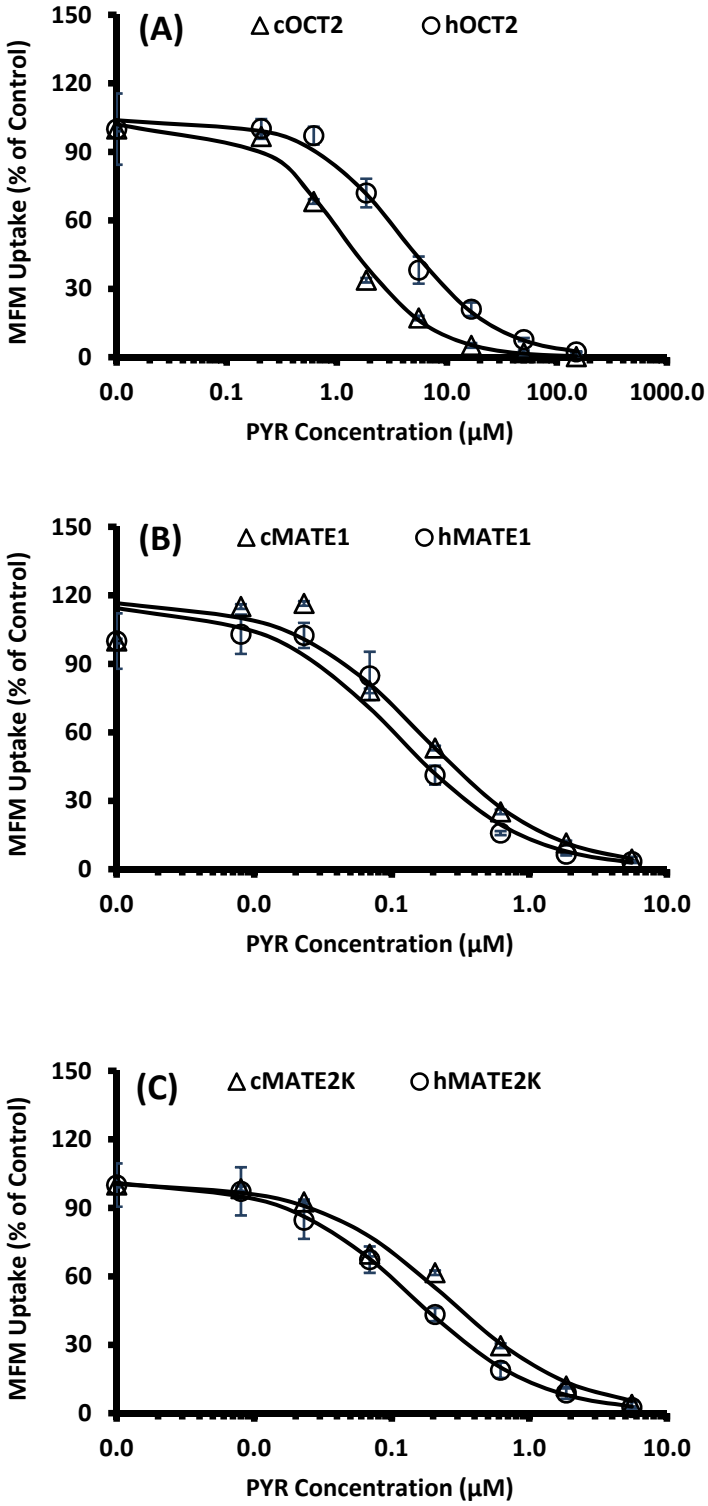

Figure 5

DMD Fast Forward. Published on November 25, 2015 as DOI: 10.1124/dmd.115.066852
This article has not been copyedited and formatted. The final version may differ from this version.

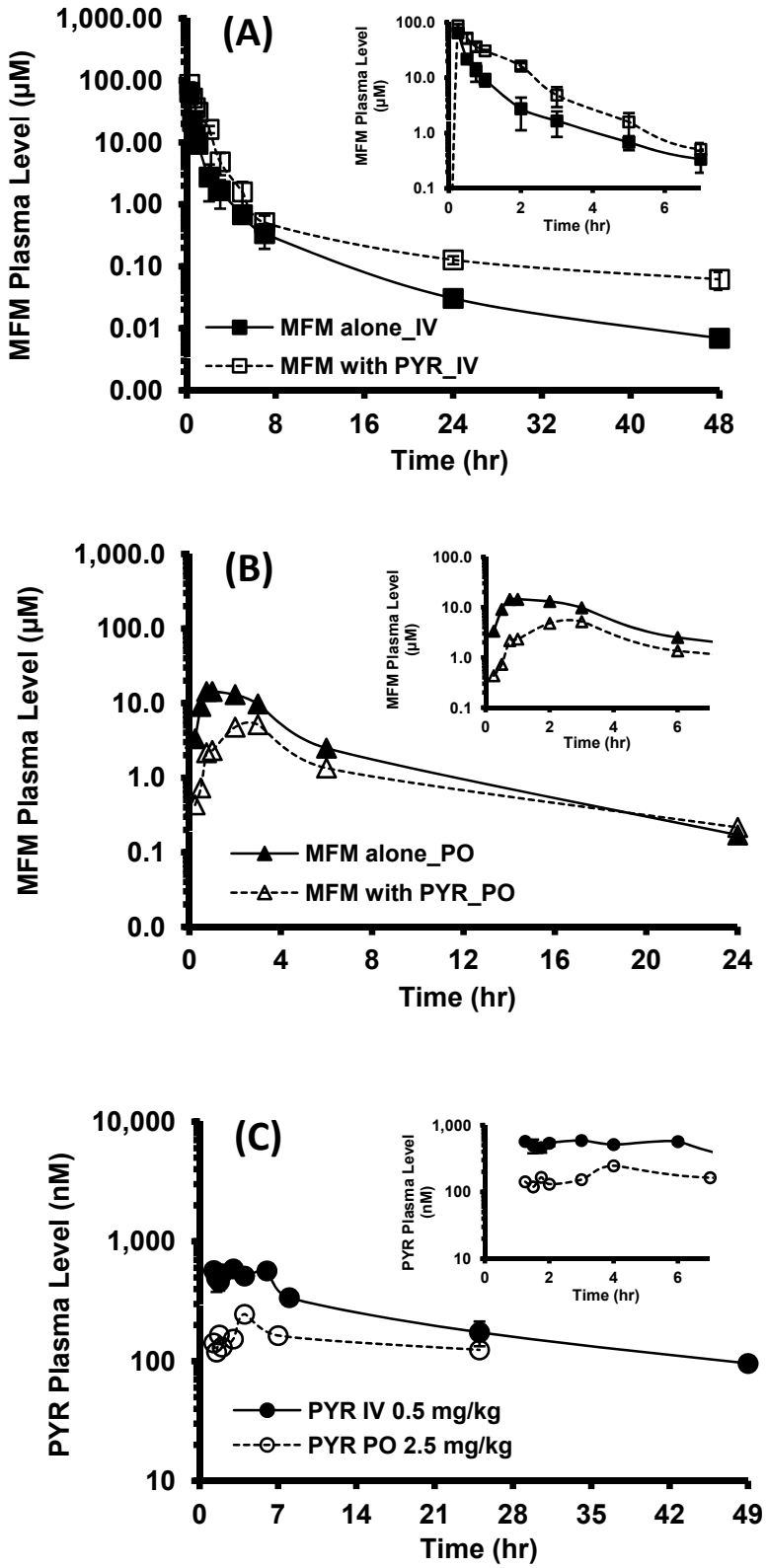

Figure 6

DMD Fast Forward. Published on November 25, 2015 as DOI: 10.1124/dmd.115.066852
This article has not been copyedited and formatted. The final version may differ from this version.

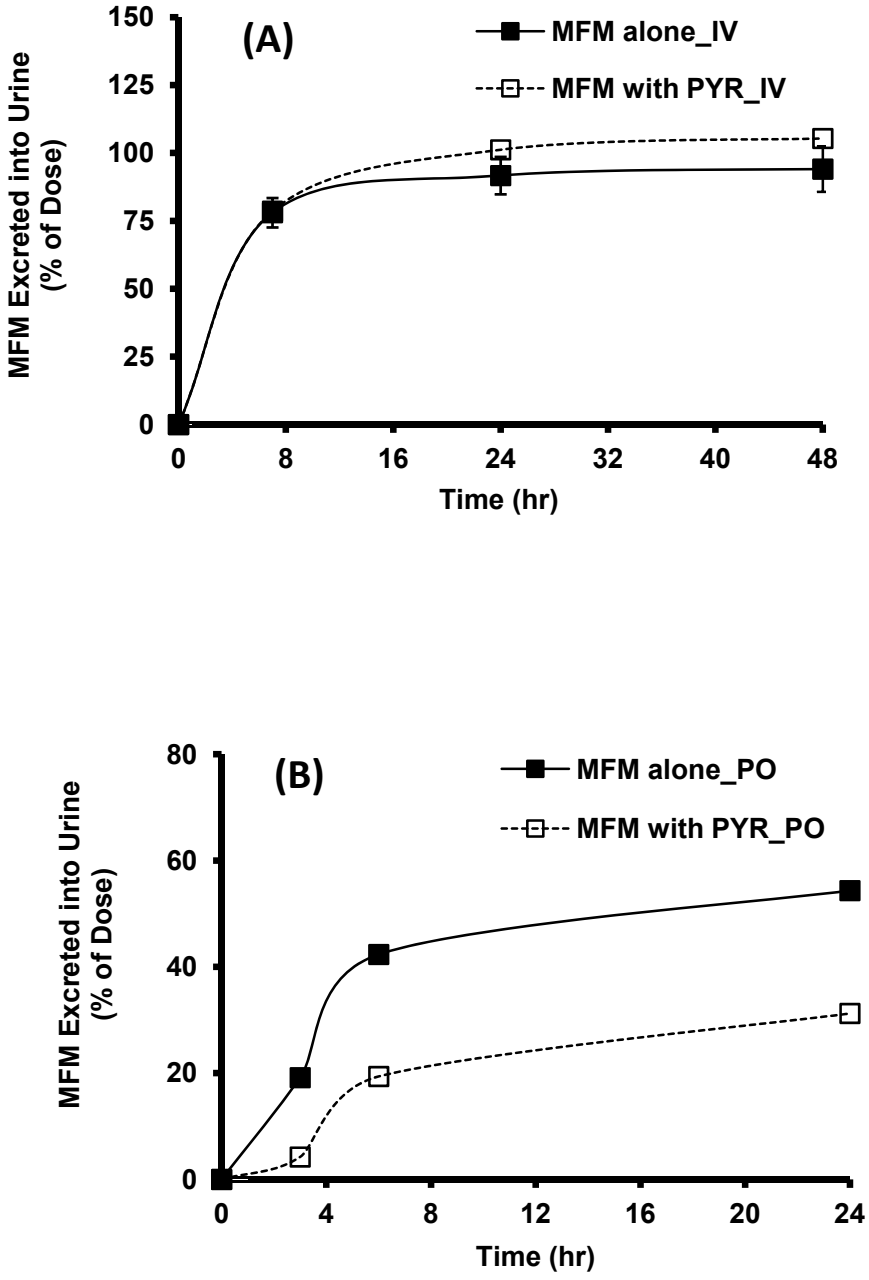

Figure 7

Supplementary Materials and Figures

Cynomolgus Monkey as a Clinically Relevant Model to Study Transport Involving Renal Organic Cation Transporters: In Vitro and In Vivo Evaluation

Hong Shen, Tongtong Liu, Hao Jiang, Craig Titsch, Kristin Taylor, Hamza Kandoussi, Xi Qiu, Cliff Chen, Sunil Sukrutharaj, Kathy Kuit, Gabe Mintier, Prasad Krishnamurthy, R. Marcus Fancher, Jianing Zeng, A. David Rodrigues, Punit Marathe, and Yurong Lai

Supplementary Material

Cloning of cOCT2, cMATE1 and cMATE2K, and Stable Transfection in HEK 293 Cells. The full-length cDNAs of cOCT2, cMATE1 and cMATE2K were cloned based on a reverse transcription polymerase chain reaction (RT-PCR) strategy as described previously (Shen et al., 2013a). Total kidney RNA pooled from 3 Mauritian cynomolgus monkeys was annealed with oligo(dT)18, and first strand cDNA synthesis was carried out with reverse transcriptase and used as a template for PCR. The following PCR primers were designed according to conserved nucleotide sequences outside the coding frames among the available transporter sequences. OCT2: 5'-GGG TTT GTG CTG AGC TGG C-3' (forward primer), 5'-GGT TGA TAG GGC TCA GGG GTA AG-3' (reverse primer); MATE1: 5'-CAG CGC GCC AGT CAC ATG-3' (forward primer), 5'-GAC TTT CTT TCC TGC CAC GTC A-3' (reverse primer); MATE2k: 5'-AGG CAG GGG ACA ACT CAC TGG-3' (forward primer), 5'-GGG AGA CCG TGG TGT GTT TG-3' (reverse primer). The cDNA products were cloned into vector pJet1.2 (Fermentas) and the sequences were verified by DNA sequencing. The monkey transporter cDNA gene sequences were deposited in National Center for Biotechnology Information (NCBI) GenBank with accession numbers of KP731382, KP731383, and KP731384 for cOCT2, cMATE1 and cMATE2K, respectively. The cDNAs including the open reading frame were subcloned into the Gateway entry vector pDONR221 (Invitrogen-Life Technologies, Carlsbad, CA). The newly generated entry vectors were finally recombined into a Gateway-adapted version of the expression vector pcDNA5/FRT/TO using the Gateway LR clonase II according to the manufacturer's protocol (Invitrogen-Life Technologies, Carlsbad, CA), and the sequences of the expression constructs were confirmed by DNA sequencing.

Stable transfection of HEK cells with cOCT2, cMATE1 or cMATE2K was carried out using the Flp-In expression system as described previously (Shen et al., 2013b). In brief, HEK 293 Flp-In cells were seeded into a 6-well plate at a density of 0.1 million cells/cm^2 in Dulbeccos's modified eagle's medium supplemented with 10% fetal bovine serum, 0.1 mM nonessential amino acids, and 2 mM L-glutamine,

on a 6-well plate. After overnight-culture, the cells reached approximately 20 to 30% confluence, and are actively proliferating. Lipofectamine 2,000 reagent (10 μL) was diluted in 250 μL of serum-free Opti-MEM I medium and incubated at room temperature for 5 min. The 250 μL of serum-free Opti-MEM I medium containing plasmid DNA (0.4 μg of recombinant plasmid plus 3.6 μg of pOG44 plasmid) was added to the Lipofectamine mixture and incubated for an additional 20 min at room temperature. The DNA-Lipofectamine mixture was then added dropwise to the cells, and the cells were incubated at 37°C for approximately 6 hr before the medium was replaced by standard culture medium without antibiotics to reduce Lipofectamine-induced cytotoxicity. After being cultured for two days, the transfected cells were then trypsinized and seeded in 100 x 20 mm dishes and selected with Hygromycin B (0.2 mg/mL). Media were changed every 3 to 4 days until hygromycin-resistant colonies formed approximately 10 days after transfection. Clones of cells were picked and seeded in 24-well plate, and amplified. Then, the uptake of [^{3}H]MPP^{+} and [^{14}C]MFM into cells was measured, leading to the identification of clones overexpressing cOCT2, cMATE1 or cMATE2K which are transport-competent toward the prototypical substrates. The mRNA and protein expression were verified by RT-PCR and liquid chromatography coupled with tandem mass spectrometry (LC-MS/MS), respectively.

References

Shen H, Yang Z, Mintier G, Han YH, Chen C, Balimane P, Jemal M, Zhao W, Zhang R, Kallipatti S, Selvam S, Sukrutharaj S, Krishnamurthy P, Marathe P and Rodrigues AD (2013a) Cynomolgus monkey as a potential model to assess drug interactions involving hepatic organic anion transporting polypeptides: in vitro, in vivo, and in vitro-to-in vivo extrapolation. *J Pharmacol Exp Ther* 344: 673-685.

Shen H, Yang Z, Zhao W, Zhang Y and Rodrigues AD (2013b) Assessment of vandetanib as an inhibitor of various human renal transporters: inhibition of multidrug and toxin extrusion as a possible

mechanism leading to decreased cisplatin and creatinine clearance. *Drug Metab Dispos* 41: 2095-2103.

Supplementary Figure 1
Alignment of the predicted amino acid sequences of cynomolgus (Cyno) and human (Human) organic cation transporters. The highlighted areas denote the difference between the sequences of cynomolgus monkey and human for OCT2 (A), MATE1 (B), and MATE2K (C). cOCT2, cMATE1, and cMATE2K have been deposited in GenBank (Accession Nos. KP731382, KP731383, and KP731384, respectively)

Supplementary Figure 1A (OCT2)

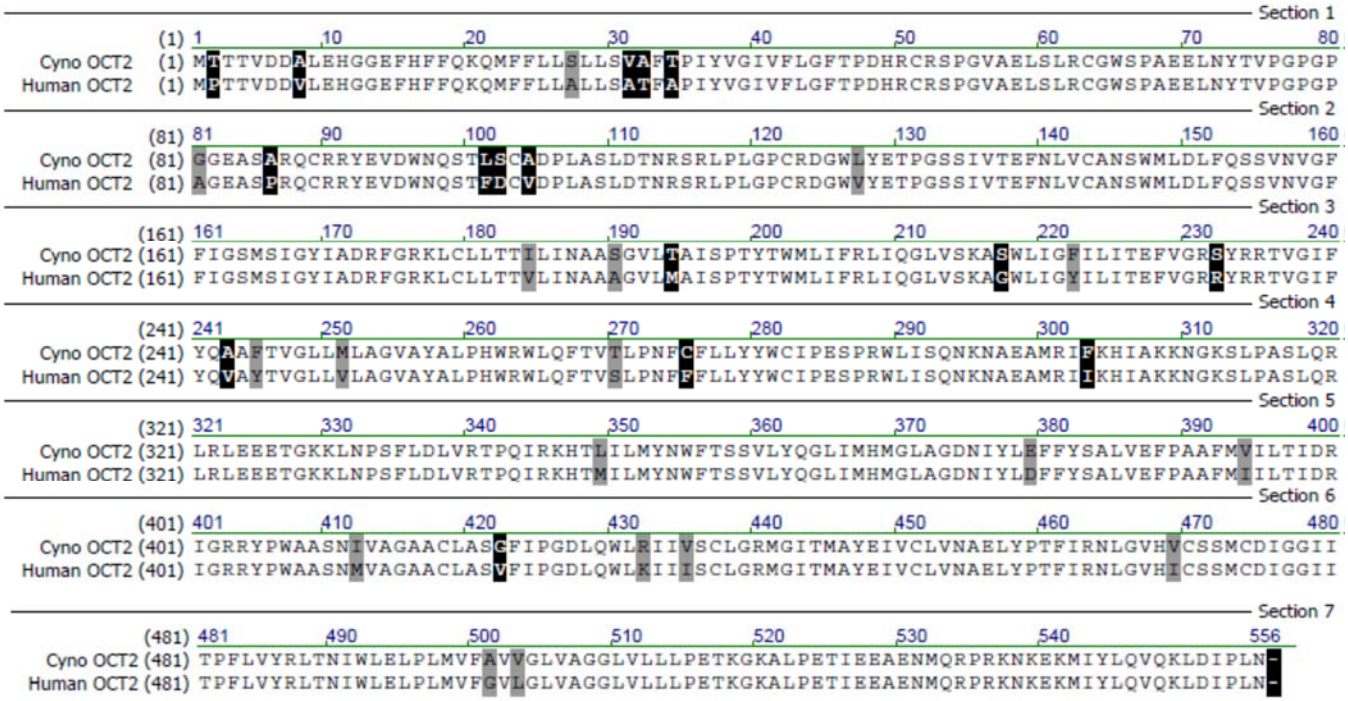

Supplementary Figure 1B (MATE1)

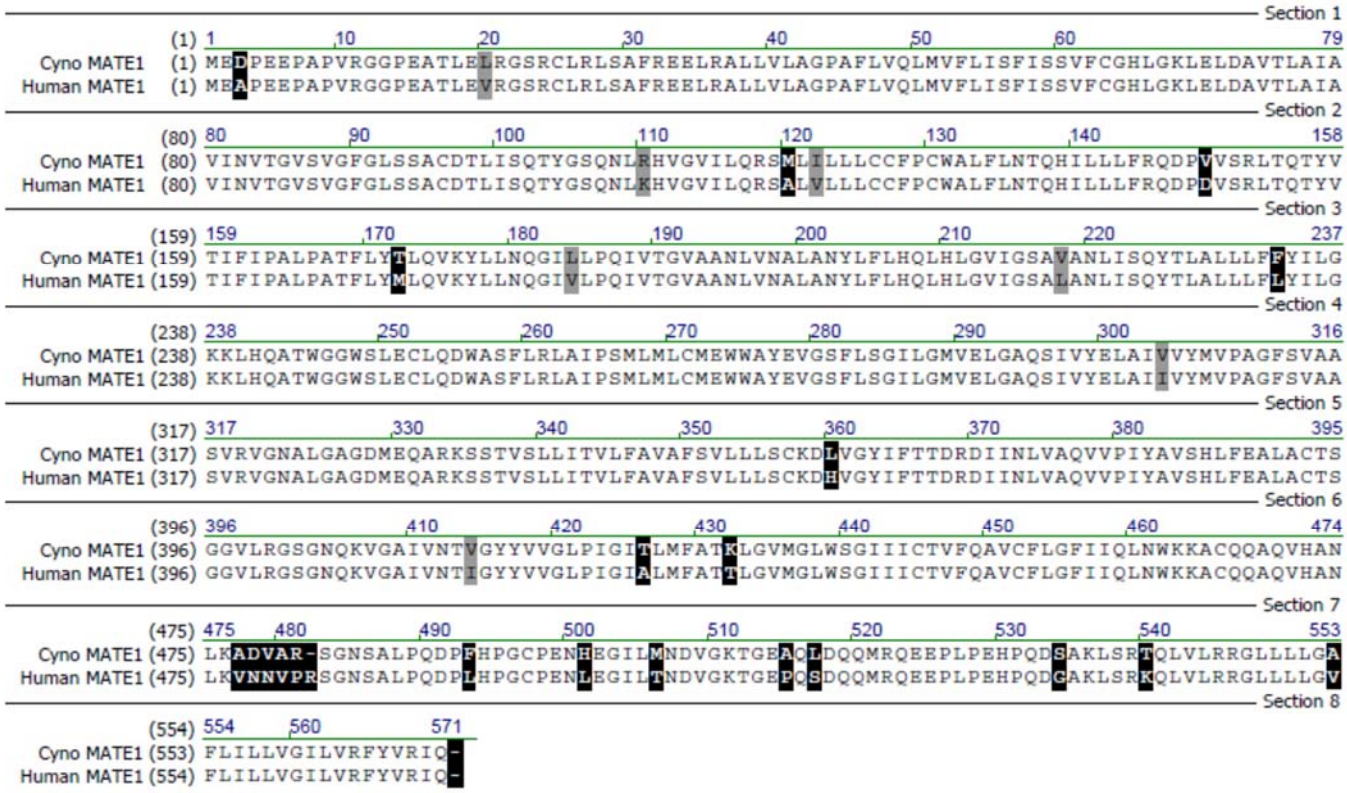

Supplementary Figure 1C (MATE2K)

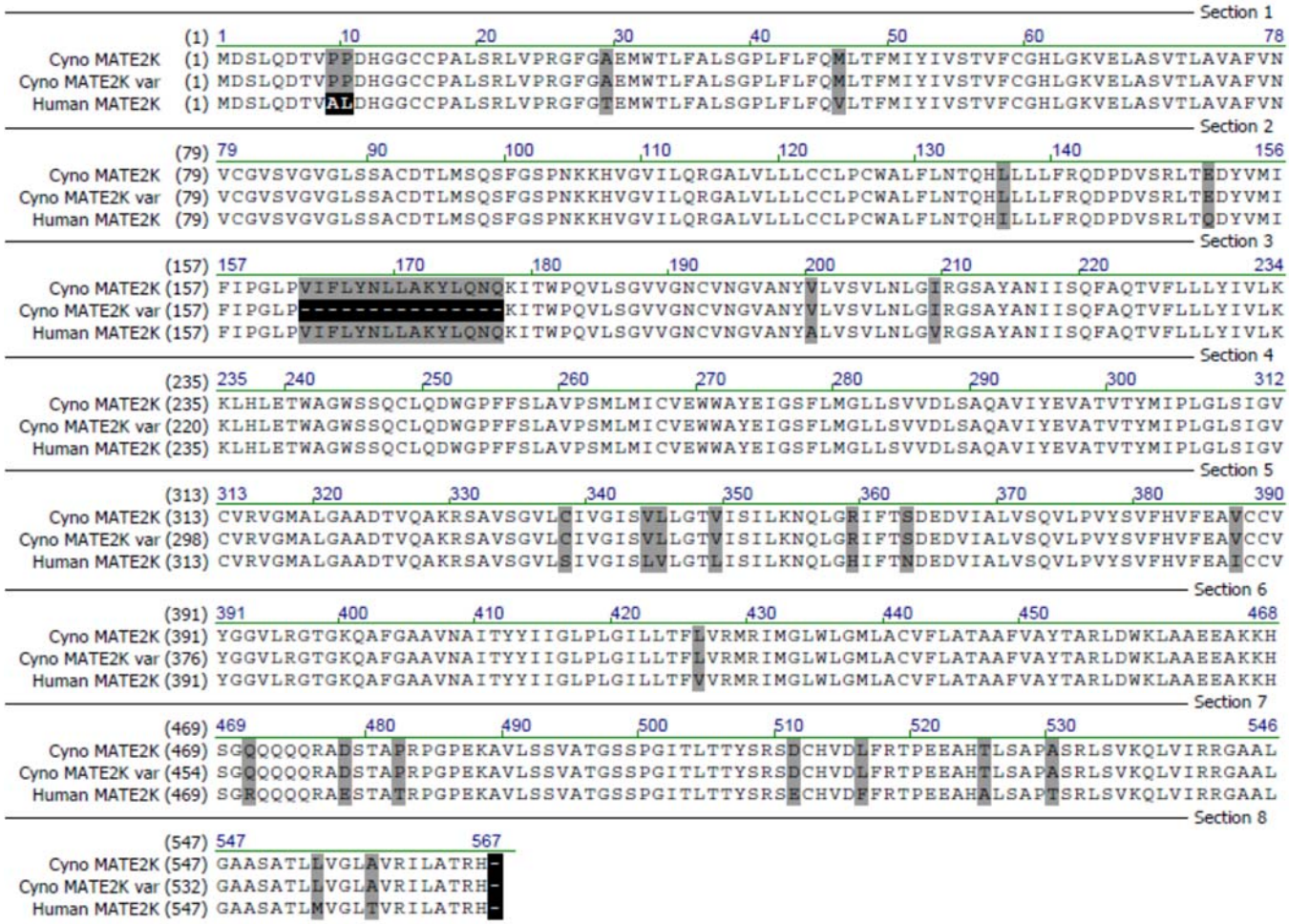

Supplementary Figure 2
Comparison of uptake of 1 μM [^{14}C]MFM (A) and [^{3}H]MPP^{+} (B) into HEK 293 cells stably expressing hMATE2k, full-length cMATE2K, deleted cMATE2K, or vector control. Uptake was performed by incubating cells with [^{14}C]MFM or [^{3}H]MPP^{+} dissolved in HBSS buffer supplemented with 10 mM HEPES (pH 8.4) at 37 ˚C as described under *Materials and Methods* for 2 min. Data are expressed as mean ± SD (n = 3)

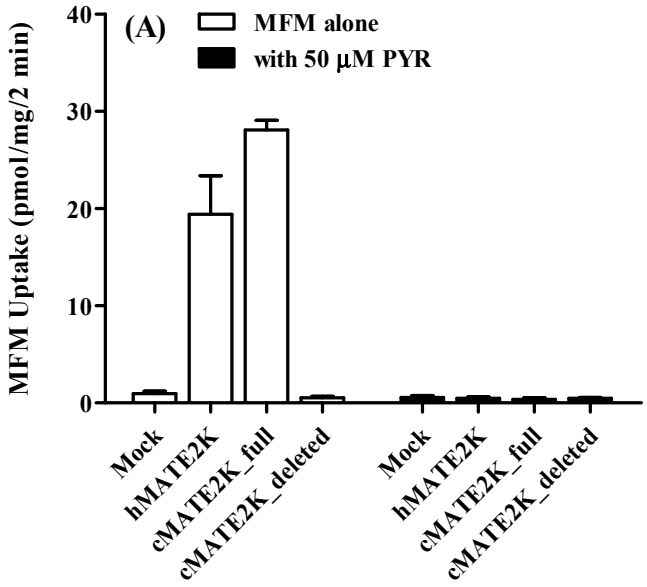

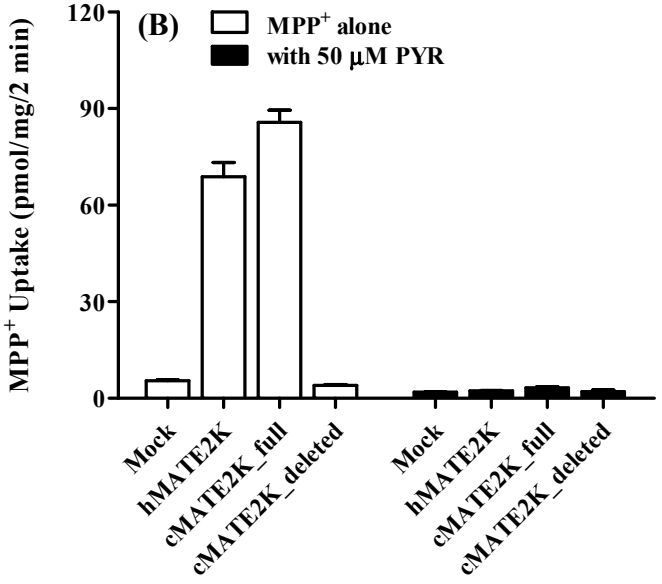

Supplementary Figure 3
Comparison of 6 compounds (PYR, CMD, QD, VDN, KCZ, and IPM) as inhibitors of cynomolgus monkey and human OCT2, MATE1, and MATE2K (*IC*$_{50}$s reported in Table 3). The solid and dotted lines represent the line of unity and the 33 to 300% range of the observed *IC*$_{50}$, respectively.

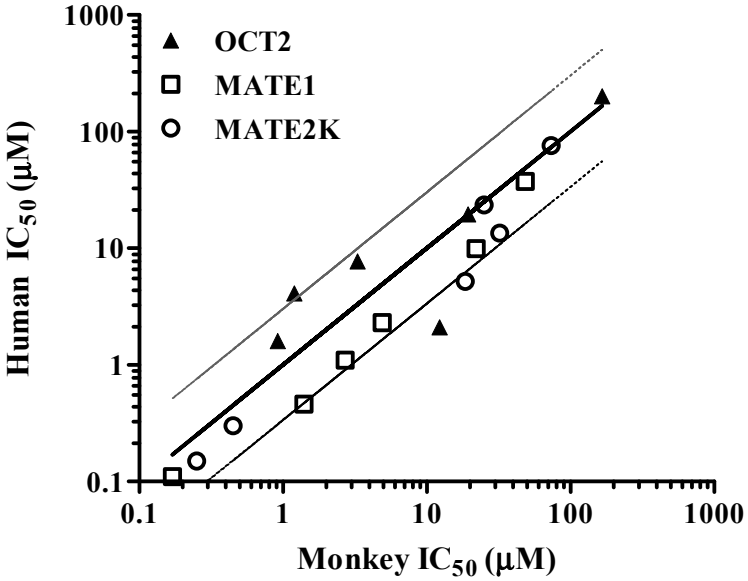

Supplementary Figure 4

Comparison of the testing of vandetanib as an inhibitor of cynomolgus monkey (A) and human MATE1 (B) on two different occasions. Increasing concentrations of VDT (0.02-11.1 µM) were added simultaneously with 2 µM [^{14}C]MFM for 2 min incubation (linear range). Extracellular pH was 8.4. The extent of inhibition of transporter-mediated uptake is expressed as a percentage of the uptake in the absence of inhibitor. Nonlinear regression analysis of the data was used to determine apparent IC_{50} values. Data are shown as mean ± SD (n = 3).